JOURNAL OF GEOPHYSICAL RESEARCH, VOL. 117, D24302, doi:10.1029/2012JD018236, 2012

Volatile organic compounds (VOCs) in urban air: How chemistry affects the interpretation of positive matrix factorization (PMF) analysis

Bin Yuan,[1] Min Shao,[1] Joost de Gouw,[2,3] David D. Parrish,[2] Sihua Lu,[1] Ming Wang,[1]
Limin Zeng,[1] Qian Zhang,[1] Yu Song,[1] Jianbo Zhang,[1] and Min Hu[1]

Received 3 June 2012; revised 27 October 2012; accepted 29 October 2012; published 28 December 2012.

[1] Volatile organic compounds (VOCs) were measured online at an urban site in Beijing in August–September 2010. Diurnal variations of various VOC species indicate that VOCs concentrations were influenced by photochemical removal with OH radicals for reactive species and secondary formation for oxygenated VOCs (OVOCs). A photochemical age-based parameterization method was applied to characterize VOCs chemistry. A large part of the variability in concentrations of both hydrocarbons and OVOCs was explained by this method. The determined emission ratios of hydrocarbons to acetylene agreed within a factor of two between 2005 and 2010 measurements. However, large differences were found for emission ratios of some alkanes and C8 aromatics between Beijing and northeastern United States secondary formation from anthropogenic VOCs generally contributed higher percentages to concentrations of reactive aldehydes than those of inert ketones and alcohols. Anthropogenic primary emissions accounted for the majority of ketones and alcohols concentrations. Positive matrix factorization (PMF) was also used to identify emission sources from this VOCs data set. The four resolved factors were three anthropogenic factors and a biogenic factor. However, the anthropogenic factors are attributed here to a common source at different stages of photochemical processing rather than three independent sources. Anthropogenic and biogenic sources of VOCs concentrations were not separated completely in PMF. This study indicates that photochemistry of VOCs in the atmosphere complicates the information about separated sources that can be extracted from PMF and the influence of photochemical processing must be carefully considered in the interpretation of source apportionment studies based upon PMF.

Citation: Yuan, B., et al. (2012), Volatile organic compounds (VOCs) in urban air: How chemistry affects the interpretation of positive matrix factorization (PMF) analysis, *J. Geophys. Res.*, *117*, D24302, doi:10.1029/2012JD018236.

1. Introduction

[2] Volatile organic compounds (VOCs) play important roles in the atmosphere as precursors of ground-level ozone and secondary organic aerosols (SOA) [*Hester*, 1995; *Koppmann*, 2007; *Seinfeld and Pandis*, 1998]. Thus, knowing the sources of VOCs is crucial for abatement strategies of ozone and particle pollution. The main technique in source appointments of VOCs is applying receptor models to ambient measurement data [*Song et al.*, 2008]. Receptor models are developed to identify and quantify source contributions to VOCs concentrations based on intrinsic statistical features of measured data [*Watson et al.*, 2001]. Receptor models also provide an approach to evaluate bottom-up emission inventories [*Morino et al.*, 2011], which are difficulty to establish and have large uncertainties [*Zhang et al.*, 2009].

[3] As a receptor model, positive matrix factorization (PMF) has been widely used in source appointments of VOCs [*Paatero*, 1997], partially due to the fact that no a priori knowledge of source profiles is required. Most of the PMF studies were applied to nonmethane hydrocarbons (NMHCs). Recently, more work incorporating oxygenated VOCs (OVOCs) has been reported [*Bon et al.*, 2011; *Gaimoz et al.*, 2011; *Shim et al.*, 2007; *Vlasenko et al.*, 2010]. One goal of these studies was the separation of OVOCs contributions from primary emissions and secondary formation [*Bon et al.*, 2011; *Vlasenko et al.*, 2009].

[4] Receptor models assume that no chemical reaction occurs during transport from the sources to the measurement

---

[1] State Joint Key Laboratory of Environmental Simulation and Pollution Control, College of Environmental Sciences and Engineering, Peking University, Beijing, China.

[2] Chemical Sciences Division, NOAA ESRL, Boulder, Colorado, USA.

[3] Also at Cooperative Institute for Research in Environmental Sciences, University of Colorado Boulder, Boulder, Colorado, USA.

Corresponding author: M. Shao, State Joint Key Laboratory of Environmental Simulation and Pollution Control, College of Environmental Sciences and Engineering, Peking University, Beijing 100871, China. (mshao@pku.edu.cn)

©2012. American Geophysical Union. All Rights Reserved.
0148-0227/12/2012JD018236

site. However, this assumption is commonly violated, since VOCs are removed at different rates by reactions with the OH radical, NO_3 radical and ozone, from the time that they are emitted into the atmosphere. Several approaches have attempted to address this problem in source appointments of NMHCs. One method considered only VOCs species with low reactivities in receptor models (e.g., less reactive than toluene in *Fujita* [2001]). However, highly reactive species do play important roles as OH reaction partners and in ozone, SOA formation in the atmosphere [*Shao et al.*, 2009]. Another method used empirical parameters to correct the influences of photochemistry on source profiles [*Na and Kim*, 2007] or measured concentrations [*Lanz et al.*, 2008; *Latella et al.*, 2005; *Shao et al.*, 2011]. In addition, none of these methods can be applied to OVOCs, due to secondary formation that is an important source for these compounds. In fact, two PMF studies including OVOCs in PMF analysis indicated that long-lived species (e.g., benzene, acetylene) appeared in the factors associated with secondary formation of OVOCs [*Bon et al.*, 2011; *Slowik et al.*, 2010]. These results suggested that extracted PMF factors may not be easily assigned to individual sources [*Shim et al.*, 2007]. However, this information is not well recognized by the research community. To our knowledge, the independences of PMF resolved factors and the validity of assignment of particular factors to specific sources have not been systematically explored in the literature.

[5] Air quality in Beijing, the host of Olympic Games in 2008, has attracted much attention from the public and scientists, due to the severe air pollution problems [*Streets et al.*, 2007], including high ozone concentrations [*Wang et al.*, 2006]. Observation-based model (OBM) showed that ozone concentrations are mainly controlled by VOCs emissions in Beijing, particularly at urban sites [*Liu et al.*, 2012; *Lu et al.*, 2010; *Shao et al.*, 2009]. The sources of VOCs in Beijing are appointed by different receptor models (CMB, PMF and UNMIX) [*Song et al.*, 2007, 2008; *Wang et al.*, 2010a]. Vehicular emissions associated with gasoline evaporation and solvent use are the most important sources for VOCs in Beijing [*Shao et al.*, 2009; *Wang et al.*, 2010a].

[6] VOCs concentrations were measured using online instruments at an urban site in Beijing in the summer of 2010. The high-resolution VOCs data set with tens of individual species provides an opportunity to conduct a critical evaluation of a PMF analysis designed to apportion the VOCs to their sources. Diurnal variations of different VOCs species are examined to gain a qualitative picture of the sources and sinks that determine the measured VOCs concentrations, and a photochemical age-based parameterization method is used to quantify the VOCs evolution in the atmosphere and also to determine the relative emissions of the VOCs. Finally, a PMF analysis is applied to the data set and the meanings of the extracted PMF factors are investigated in detail.

2. Measurements

2.1. VOCs Measurements

[7] VOCs were measured at an urban site (39.99°N, 116.31°E) in Beijing in August–September 2010. The sampling site was on the top of a six-story building on Peking University (PKU) campus. The sampling site was also one of the supersites for the series of CAREBeijing campaigns and it has been described extensively in several published papers [*Shao et al.*, 2009; *Wang et al.*, 2010a]. Five techniques were used for VOCs measurements, including online GC-MS/FID, PTR-MS, online gas chromatography with flame ionization detection and photo ionization detection (GC-FID/PID), canister collection followed by off-line GC-MS/FID analysis and 2,4-dinitrophenylhydrazine (DNPH) cartridges. In this study, the measured data from online GC-MS/FID and PTR-MS are used.

[8] The online GC-MS/FID was a custom built two-channel system, which was used to measure C2–C10 hydrocarbons and selected C2–C4 carbonyls. This system was described in *X. L. Liu et al.* [2009]. Briefly, most C2–C5 hydrocarbons were measured by the FID channel with a PLOT column (15 m × 0.32 mm ID, J&W Scientific), and the MS channel analyzed a range of other compounds using a DB-624 column (30 m × 0.25 mm ID, J&W Scientific). The measured hydrocarbon species by GC-MS/FID are listed in Table 1. Several OVOCs species are also measured by the MS channel, including acetone, propanal, n-butanal, methyl ethyl ketone (MEK), methyl vinyl ketone (MVK) and methacrolein (MACR). The two channels have their own inlets, cold traps and GC separation columns, but they share one cryogenic source and programmed temperature procedure. After removal of water vapor, VOCs were trapped at $-155°C$ in a deactivated quartz capillary column (15 cm × 0.53 mm ID) and a PLOT capillary column (15 cm × 0.53 mm ID) for the MS channel and the FID channel, respectively. Ascarite II was used to remove CO_2 and ozone before the FID channel, whereas a Na_2SO_3 trap was used to remove ozone in the MS channel. The system was calibrated at multiple concentrations in the range of 0–8 ppb by two gas standards provided by Spectra Gases Inc., USA and Apel-Riemer Environmental Inc., USA. Detection limits for various compounds were in the range of 0.002–0.070 ppbv.

[9] A commercial high-sensitivity (HS) PTR-MS (Ionicon Analytik, Innsbruck, Austria) measured a subset of VOCs species. In PTR-MS, VOCs react with H_3O^+ in the drift tube to form $VOC{\cdot}H^+$ ions and the ions are detected by a quadruple mass spectrometer [*de Gouw and Warneke*, 2007]. During the campaign, the system was run at multiple ion mode with a total of 24 masses recorded, including H_3O^+ (at its isotope m/z 21) and $H_3O^+(H_2O)$ (at m/z 39). Most of the masses were recorded for 1 s in every cycle, except m/z 21 (0.2 s) and m/z 137 (2 s). Background signals were measured by passing ambient air through a Platinum coated-wool trap (Shimadzu Inc., Japan) heated to 350°C for 30 cycles after every 300 cycles of ambient measurements. Aromatics masses (m/z 79 for benzene, m/z 93 for toluene, m/z 105 for styrene, m/z 107 for C8 aromatics and m/z 121 for C9 aromatics), oxygenated masses (m/z 33 for methanol, m/z 45 for acetaldehyde, m/z 59 for acetone, m/z 71 for MVK+MACR and m/z 73 for MEK), isoprene (m/z 69) and acetonitrile (m/z 42) were calibrated by a cylinder gas standard (provided by Apel-Riemer Environmental Inc., USA). Formaldehyde (m/z 31), formic acid (m/z 47), acetic acid (m/z 61), monoterpenes (m/z 81 and m/z 137) were calibrated by permeation tubes obtained from Kin-Tek, USA. Formaldehyde was calibrated at a range of humidities (0–25 m mol/mol) to account for the sensitivity dependence

Table 1. Correlation Coefficients Between Measured and Calculated Hydrocarbon Concentrations in Beijing in 2010 and Emission Ratios (ERs) of Hydrocarbons Relative to Acetylene and CO in Beijing[a]

Species	R	ERs in 2010 (ppb [ppb C_2H_2]$^{-1}$)	ERs in 2010 (ppb [ppm CO]$^{-1}$)	ERs in 2005 (ppb [ppb C_2H_2]$^{-1}$)
Ethane	0.81	1.03 ± 0.03	4.02 ± 0.18	0.55 ± 0.01
Ethylene	0.84	1.24 ± 0.03	4.86 ± 0.21	0.92 ± 0.02
Propane	0.81	0.90 ± 0.03	3.54 ± 0.16	0.73 ± 0.02
Propene	0.74	0.31 ± 0.01	1.20 ± 0.06	0.30 ± 0.01
Isobutane	0.81	0.67 ± 0.02	2.63 ± 0.12	0.52 ± 0.01
n-Butane	0.81	0.71 ± 0.02	2.76 ± 0.12	0.60 ± 0.01
Acetylene	N/A	N/A	3.92 ± 0.13	
1-Butene	0.70	0.24 ± 0.01	0.95 ± 0.05	0.30 ± 0.01
cis-2-Butene	0.77	0.04 ± 0.00	0.14 ± 0.01	0.11 ± 0.01
Isopentane	0.84	0.63 ± 0.02	2.48 ± 0.11	0.81 ± 0.02
n-Pentane	0.83	0.38 ± 0.01	1.48 ± 0.07	0.35 ± 0.01
1-Pentene	0.67	0.03 ± 0.00	0.11 ± 0.01	
trans-2-Pentene	0.53	0.03 ± 0.00	0.11 ± 0.01	
cis-2-Pentene	0.51	0.01 ± 0.00	0.05 ± 0.00	
2,2-DMbutane	0.69	0.01 ± 0.00	0.04 ± 0.00	
2,3-DMbutane	0.75	0.02 ± 0.00	0.09 ± 0.00	
2-Methylpentane	0.80	0.11 ± 0.00	0.44 ± 0.02	
Cyclopentane	0.80	0.03 ± 0.00	0.14 ± 0.01	
3-Methylpentane	0.80	0.17 ± 0.01	0.67 ± 0.03	
1-Hexene	0.57	0.02 ± 0.00	0.06 ± 0.00	
n-Hexane	0.63	0.16 ± 0.01	0.62 ± 0.04	0.13 ± 0.01
2,4-DMpentane	0.70	0.01 ± 0.00	0.05 ± 0.00	
MCpentane	0.75	0.11 ± 0.00	0.43 ± 0.02	
2-Methylhexane	0.85	0.07 ± 0.00	0.26 ± 0.01	
Cyclohexane	0.57	0.06 ± 0.00	0.22 ± 0.02	
3-Methylhexane	0.82	0.10 ± 0.00	0.37 ± 0.02	
Benzene	0.87	0.46 ± 0.01	1.80 ± 0.07	0.28 ± 0.00
2,2,4-TMPentane	0.62	0.01 ± 0.00	0.03 ± 0.00	
n-Heptane	0.86	0.07 ± 0.00	0.27 ± 0.01	
MChexane	0.86	0.04 ± 0.00	0.16 ± 0.01	
2,3,4-TMPentane	0.73	0.00 ± 0.00	0.01 ± 0.00	
2-Methylheptane	0.88	0.02 ± 0.00	0.08 ± 0.00	
3-Methylheptane	0.86	0.02 ± 0.00	0.07 ± 0.00	
Toluene	0.82	1.00 ± 0.03	3.93 ± 0.17	0.63 ± 0.01
Octane	0.88	0.03 ± 0.00	0.12 ± 0.00	
Ethylbenzene	0.85	0.54 ± 0.01	2.11 ± 0.09	0.29 ± 0.01
n-Nonane	0.82	0.03 ± 0.00	0.12 ± 0.01	
m+p-Xylene	0.91	1.11 ± 0.02	4.34 ± 0.17	0.67 ± 0.01
o-Xylene	0.91	0.38 ± 0.01	1.50 ± 0.06	0.28 ± 0.00
Styrene	0.75	0.11 ± 0.00	0.43 ± 0.02	
i-Propylbenzene	0.66	0.02 ± 0.00	0.09 ± 0.01	
n-Propylbenzene	0.83	0.03 ± 0.00	0.12 ± 0.01	
3-Ethyltoluene	0.81	0.10 ± 0.00	0.39 ± 0.02	
4-Ethyltoluene	0.82	0.04 ± 0.00	0.17 ± 0.01	
n-Decane	0.71	0.04 ± 0.00	0.15 ± 0.01	0.06 ± 0.00
1,3,5-TMB	0.76	0.04 ± 0.00	0.18 ± 0.01	
2-ethyltoluene	0.80	0.04 ± 0.00	0.16 ± 0.01	
1,2,4-TMB	0.84	0.17 ± 0.00	0.65 ± 0.03	
1,2,3-TMB	0.84	0.05 ± 0.00	0.21 ± 0.01	
1,3-DEbenzene	0.79	0.01 ± 0.00	0.03 ± 0.00	
1,4-DEbenzene	0.83	0.05 ± 0.00	0.19 ± 0.01	
Undecane	0.75	0.02 ± 0.00	0.08 ± 0.00	

[a] Measurements from GC-MS/FID for these hydrocarbons are used. Values for ERs are expressed as "average ± standard deviation." DM, dimethyl-; DE, diethyl-; MC, methylcyclo-; TM, trimethyl-; TMB, trimethylbenzene.

on water content of the atmosphere [*Vlasenko et al.*, 2010; *Warneke et al.*, 2011].

[10] Comparisons between PTR-MS and GC-MS/FID data show good agreements for benzene, toluene, C8 aromatics, C9 aromatics, styrene, acetone and MVK+MACR, with correlation coefficients larger than 0.90 and slopes ranging from 0.7 to 1.3. Although strong correlation is obtained for MEK data between PTR-MS and GC-MS/FID, the regression slope is 1.40, which is just outside the combined uncertainty of the two instruments (30%). The correlation coefficient for isoprene is 0.84 and the regression line is $c_{\text{PTR-MS}} = 0.57 \times c_{\text{GC-MS/FID}} + 0.26$. The measurements of isoprene by PTR-MS at m/z 69 may have interferences from other species in urban areas [*de Gouw et al.*, 2003]. Isoprene data from GC-MS/FID is used in this study.

2.2. Ancillary Measurements of Other Parameters

[11] Other gases and meteorological parameters were also measured at the site. CO was measured by a commercial nondispersive infrared sensor (NDIR) based on gas filter correlation method (Thermo Environmental Instruments, TEI Inc., Model 48iTL). Ozone was measured by a commercial

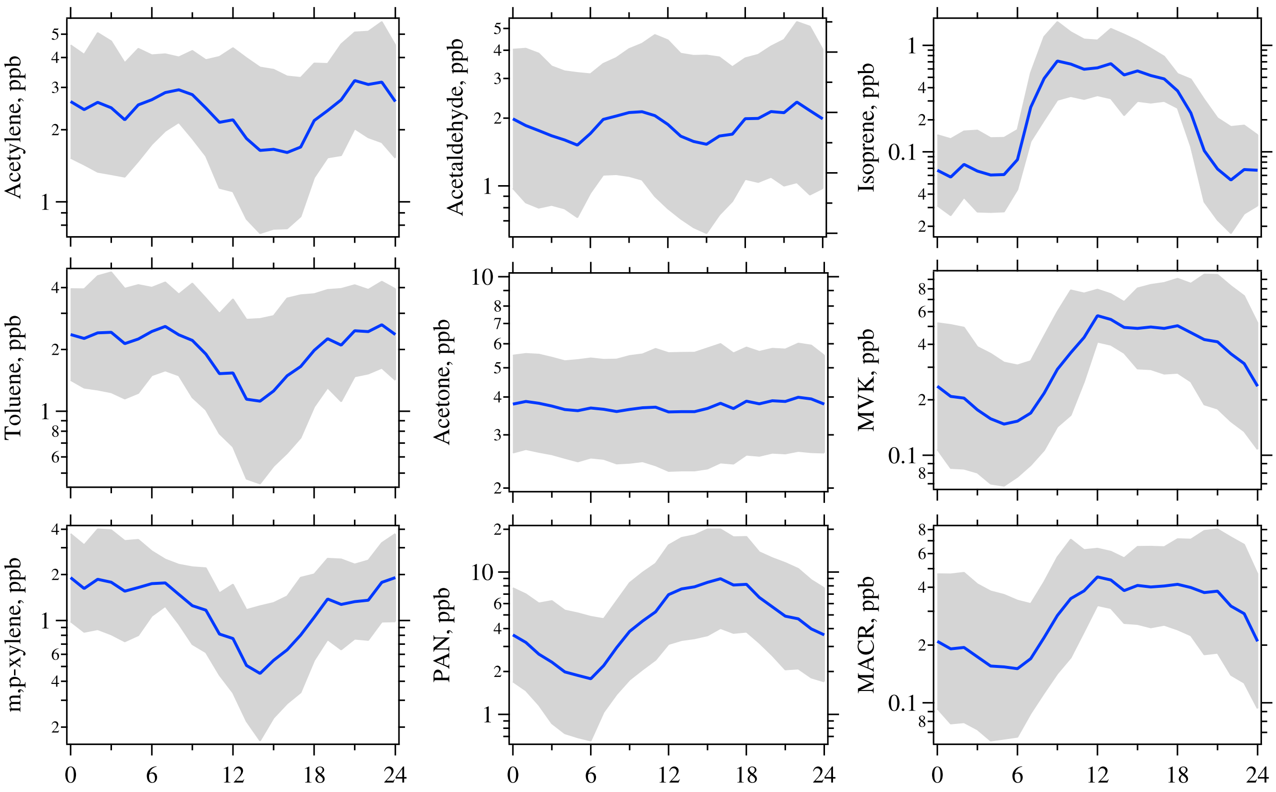

Figure 1. Diurnal variations of different VOCs and PAN. Blue lines are geometric averages, and gray areas indicate geometric standard deviations.

UV photometric analyzer (TEI, Model 49i). NO and NO_2 were measured by a chemiluminescence trace level analyzer (TEI, Model 42iTL). Temperature, relative humidity, pressure, wind speed and wind direction were recorded by an automatic weather monitoring system (Met One Instruments Inc.). Peroxyacetyl nitrate (PAN) was measured by an online gas chromatography–electron capture detection (GC-ECD) system with a time resolution of 5 min [*Wang et al.*, 2010b].

3. Results

3.1. Diurnal Variations of VOCs Species

[12] Figure 1 illustrates diurnal variations of several VOCs species. Acetylene is a hydrocarbon with relatively low reactivity. Concentrations of acetylene changed little through the day, with a small decrease in the afternoon (12:00–18:00). The diurnal profiles of acetylene reflect the combined effects of emissions cycles of various sources and variations of atmospheric boundary layer height. Toluene and m+p-xylene showed diurnal variations similar to acetylene, but the percentage of concentration reduction in the afternoon (toluene: 37%, m+p-xylene: 59%) were higher than that of acetylene (28%). The differences are consistent with the greater reactivity of toluene (5.6×10^{-12} cm^3 $molecule^{-1}$ s^{-1}) and m+p-xylene (18.9×10^{-12} cm^3 $molecule^{-1}$ s^{-1}) [*Atkinson et al.*, 2006] compared to acetylene (0.85×10^{-12} cm^3 $molecule^{-1}$ s^{-1}).

[13] The diurnal variations of PAN illustrate the time profile of formation for a secondary species. PAN concentrations increased from a minimum near sunrise to a maximum in the late afternoon, reflecting the accumulation of PAN during the photochemically active period of the day. Acetaldehyde (1.5×10^{-11} cm^3 $molecule^{-1}$ s^{-1}) has an OH rate constant comparable to m+p-xylene, but its diurnal cycle showed a small peak in the morning (around 9:00 A.M.), and did not decrease through the day to the extent of m+p-xylene. This diurnal cycle provides evidence that secondary formation is important for this highly reactive aldehyde. Acetone showed virtually no distinct diurnal variation. Acetone reacts slowly with OH similar to acetylene. Comparing the diurnal variations of acetone and acetylene suggests that acetone has sources from both primary emissions and secondary formation.

[14] Isoprene concentrations followed the solar radiation cycles as expected, with somewhat higher concentrations in the morning reflecting the smaller boundary layer depth during that time. The low concentrations (about 0.1 ppb) at night likely indicate small isoprene emissions from vehicles in Beijing. MVK and MACR, two photooxidation products of isoprene, exhibited high concentrations in the afternoon due to accumulation from oxidation of daytime isoprene and declined only slowly through the night.

3.2. Characterization of VOCs Chemistry

3.2.1. The Photochemical Age-Based Parameterization Method

[15] As shown in the discussion of diurnal variations of VOCs species, photochemical reactions played important roles in the concentrations of both NMHCs and OVOCs. Here, a photochemical age-based parameterization method is applied to describe the photochemistry of VOCs in the atmosphere. The approach selected was first introduced by

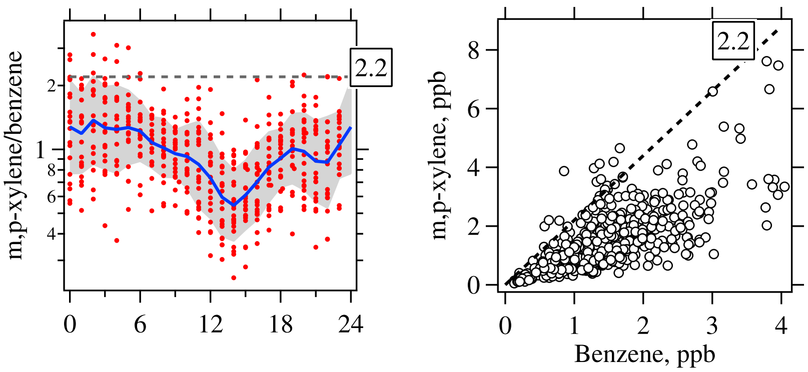

Figure 2. Concentration ratios of m+p-xylene to benzene in Beijing campaign. (left) Diurnal variations of m+p-xylene/benzene concentration ratios. Red dots are measured ratios during the campaign. Blue line indicates hourly geometric average, and gray areas are geometric standard deviations. (right) Correlation of m+p-xylene with benzene. The dashed line in both graphs show the estimated initial emission ratio of m+p-xylene/benzene (2.2).

de Gouw et al. [2005] and was applied to VOCs measurements in the northeastern U.S during the NEAQS 2002 campaign. The assumptions in the parameterization method are [*de Gouw et al.*, 2005] (1) urban and biogenic emissions are the dominant sources of VOCs in the study domain, (2) the magnitude of urban emissions is proportional to acetylene emissions, (3) the removal of VOCs is mainly due to reaction with OH radicals, (4) photochemical age could be calculated from concentration ratio of two VOCs species (m+p-xylene and benzene in this study), and (5) OVOCs emissions from biogenic sources are proportional to isoprene emissions. The assumptions (1) and (2) are reasonable, as the vehicular emissions are the dominant source of anthropogenic VOCs in Beijing [*Wang et al.*, 2010a]. The assumption (5) is also reliable as the situation in northeastern U.S. [*de Gouw et al.*, 2005]. The relative contribution of OH radical, ozone and NO_3 radical to oxidations of VOCs is investigated to test assumption (3). Measured VOCs and ozone concentrations and the modeled diurnal profile of OH radical at PKU site in August of 2007 [*Liu et al.*, 2012] are combined with NO_3 radical concentrations calculated at steady state, considering production from reaction of NO_2 with O_3 and losses from reactions of NO_3 with NO and VOCs species. The results show that OH radical accounted for more than 90% of the daily averaged loss rates of all VOCs species except monoterpenes, and support assumption (3) for all anthropogenic VOCs species during the campaign. The assumption (4) will be further discussed in the following discussion.

[16] In the parameterization method, photochemical age is used to represent the photochemical reaction time. Photochemical age can be calculated by the ratios of two hydrocarbons that react at different rates with OH [*Roberts et al.*, 1984]. In this study, we prefer to use OH exposure ($[\mathrm{OH}]\Delta t$) [*Jimenez et al.*, 2009], the product of OH radical concentration [OH] and reaction time Δt for the VOCs in the atmosphere between emission and measurement, since [OH] term and Δt term always appear in pairs in the parameterization equations of hydrocarbons and OVOCs shown below. The VOCs measurements considered here were conducted at an urban site in the midst of the emission sources, thus a VOCs pair (m+p-xylene and benzene) with large differences in OH rate constants (k_{OH}) was chosen. OH exposure is determined from the VOC concentration ratios by the following equation:

$$[\mathrm{OH}]\Delta t = \frac{1}{(k_{\mathrm{X}} - k_{\mathrm{B}})} \times \left[\ln \frac{[\mathrm{X}]}{[\mathrm{B}]}\bigg|_{t=0} - \ln \frac{[\mathrm{X}]}{[\mathrm{B}]} \right]. \qquad (1)$$

[17] The parameters k_{x} and k_{B} are rate constants of m+p-xylene (1.89×10^{-11} cm^3 $\mathrm{molecule}^{-1}$ s^{-1}) [*Atkinson et al.*, 2006] and benzene (1.22×10^{-12} cm^3 $\mathrm{molecule}^{-1}$ s^{-1}), respectively. $\frac{[\mathrm{X}]}{[\mathrm{B}]}\Big|_{t=0}$ is the initial concentration ratio of m+p-xylene/benzene in fresh emissions, i.e., the initial emission ratio before aging begins. $\frac{[\mathrm{X}]}{[\mathrm{B}]}$ is the measured concentration ratio of m+p-xylene/benzene. The limitations of using hydrocarbon ratios to calculate photochemical age or OH exposure are addressed by many studies [*McKeen et al.*, 1996; *Parrish et al.*, 2007, and references therein]. Although mixing of fresh emissions with aged air masses will introduce substantial uncertainties in the determination of photochemical age, it still provides useful measures of photochemical processing in the atmosphere [*Parrish et al.*, 2007].

[18] Diurnal variations of the measured m+p-xylene/benzene ratios during the campaign are shown in Figure 2, with higher ratios at night and lower ratios in the daytime. The initial emission ratio of m+p-xylene/benzene is estimated in three steps: (1) a linear fit is conducted to natural logarithm transformed data of m+p-xylene and benzene measured in the early morning (0:00–5:00 A.M.), (2) the regression line is extrapolated to the highest benzene concentration in this period, and (3) the initial emission ratio of m+p-xylene to benzene is calculated from the concentration ratio of m+p-xylene to benzene at this point. The initial emission ratio is calculated to be 2.2 ppb/ppb, which is close to the slope of the upper "edge" in the scatterplot. The m+p-xylene/benzene ratios of a few data points in 0:00–5:00 A.M. were higher than 2.2 ppb/ppb and are likely due to specific nearby VOCs

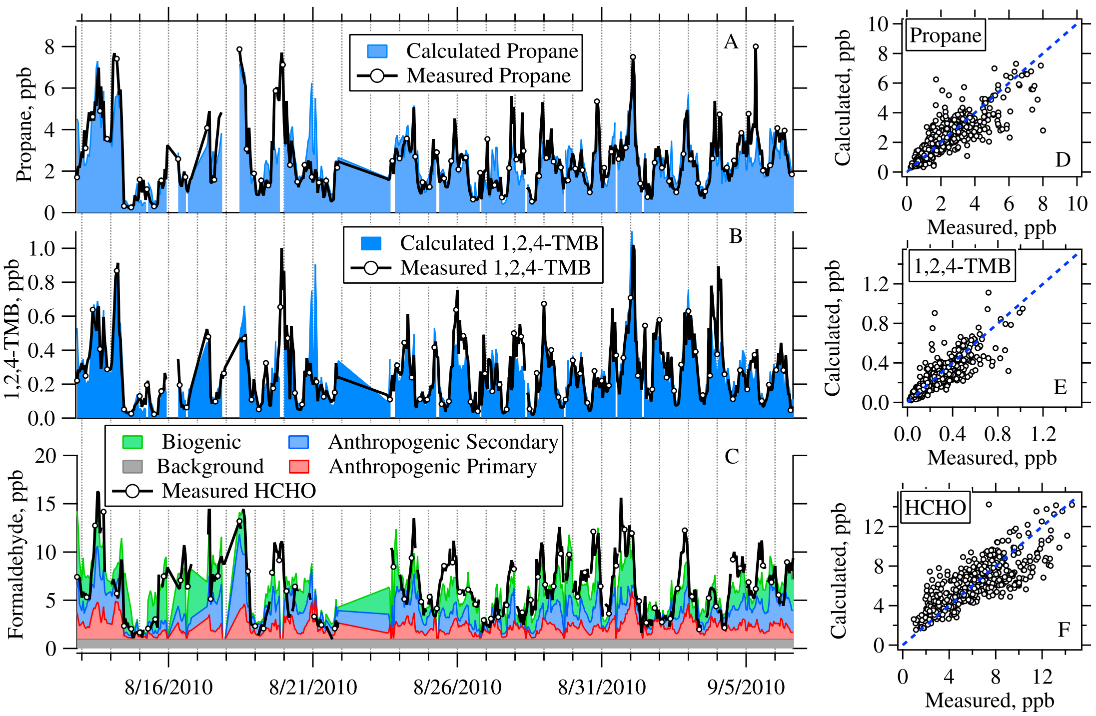

Figure 3. Comparisons of measured VOC concentrations and those calculated from the photochemical age-based parameterization method for (a) propane, (b) 1,2,4-trimethylbenzene (1,2,4-TMB), and (c) formaldehyde. Scatterplots of the calculated and measured concentrations for (d) propane, (e) 1,2,4-TMB, and (f) formaldehyde. The blue dashed lines are the 1:1 relationship.

sources with different m+p-xylene/benzene emission ratios. Uncertainties in estimating the initial emission ratio of m+p-xylene/benzene do exist and the influence to the analysis will be discussed below.

3.2.2. Chemistry and Emission Ratios of Hydrocarbons

[19] The removal of anthropogenic hydrocarbons from the atmosphere by OH oxidation can be described by [*de Gouw et al.*, 2005]:

$$[\mathrm{NMHC}] = [\mathrm{C_2H_2}] \times \mathrm{ER} \times \exp\left[-(k_{\mathrm{NMHC}} - k_{\mathrm{C_2H_2}})[\mathrm{OH}]\Delta t\right] \quad (2)$$

where [NMHC] and [C_2H_2] are concentrations of a particular NMHC species and acetylene, respectively. k_{NMHC} and $k_{\mathrm{C_2H_2}}$ are OH rate constants for the NMHC and acetylene (0.85×10^{-12} cm^3 molecule^{-1} s^{-1}). The OH exposure ([OH]Δt) is calculated from equation (1). ER is the emission ratio of the hydrocarbons relative to acetylene. ER and k_{NMHC} are treated as unknown parameters in equation (2) and determined from the regression fits [*de Gouw et al.*, 2005]. The derived values for k_{NMHC} can be compared to literature values to test the fit results. Good agreements for hydrocarbons with reactivity lower than m+p-xylene are obtained, but the fitting derived k_{OH} values are significantly lower than literature ones for the more reactive species. The differences can be attributed to the influence of mixing of emissions of different ages (see *de Gouw et al.* [2005] for further discussions).

[20] The fit results for propane ($k_{OH} = 1.09 \times 10^{-12}$ cm^3 molecule^{-1} s^{-1}) and 1,2,4-trimethylbenzene ($k_{OH} = 3.25 \times 10^{-11}$ cm^3 molecule^{-1} s^{-1}) [*Atkinson et al.*, 2006] are shown in Figure 3. The calculated concentrations from fitted parameters based on equation (2) followed well with measured concentrations for both low-reactive propane and highly reactive 1,2,4-trimethylbenzene, with correlation coefficients (R) of 0.81 and 0.84, respectively. The correlation coefficients (R) of measured and calculated concentrations for other hydrocarbons are shown in Table 1. For most of hydrocarbons, R are larger than 0.80. The correlations of measured and calculated concentrations for some highly reactive compounds (e.g., C4–C5 alkenes) were not as strong as other compounds, possibly due to their low measured concentrations.

[21] The determined emission ratios to acetylene for all hydrocarbons are shown in Table 1. The uncertainties in calculating emission ratios of hydrocarbons come from the measurement errors of various hydrocarbons and also the estimation of initial emission ratios of m+p-xylene/benzene for calculating OH exposure [*Warneke et al.*, 2007]. Higher (3.0) and lower (1.7) initial emission ratios of m+p-xylene/benzene were also used to calculated OH exposure and then test the uncertainties of emission ratios of hydrocarbons to acetylene. It is reasonable that a higher initial emission ratio of m+p-xylene/benzene is associated with higher emission ratios of hydrocarbons (and vice versa), consistent with the results in previous work [*Warneke et al.*, 2007]. Generally, highly reactive species are more significantly affected by the selection of the initial m+p-xylene/benzene emission ratio. The relative changes of calculated emission ratio of hydrocarbons range from −6% to 37% and from −18% to 4% for higher and lower initial emission ratio of m+p-xylene/benzene. Adding the measurement errors of hydrocarbons (10%) gives calculated uncertainties of the emission ratios that are less than 50%.

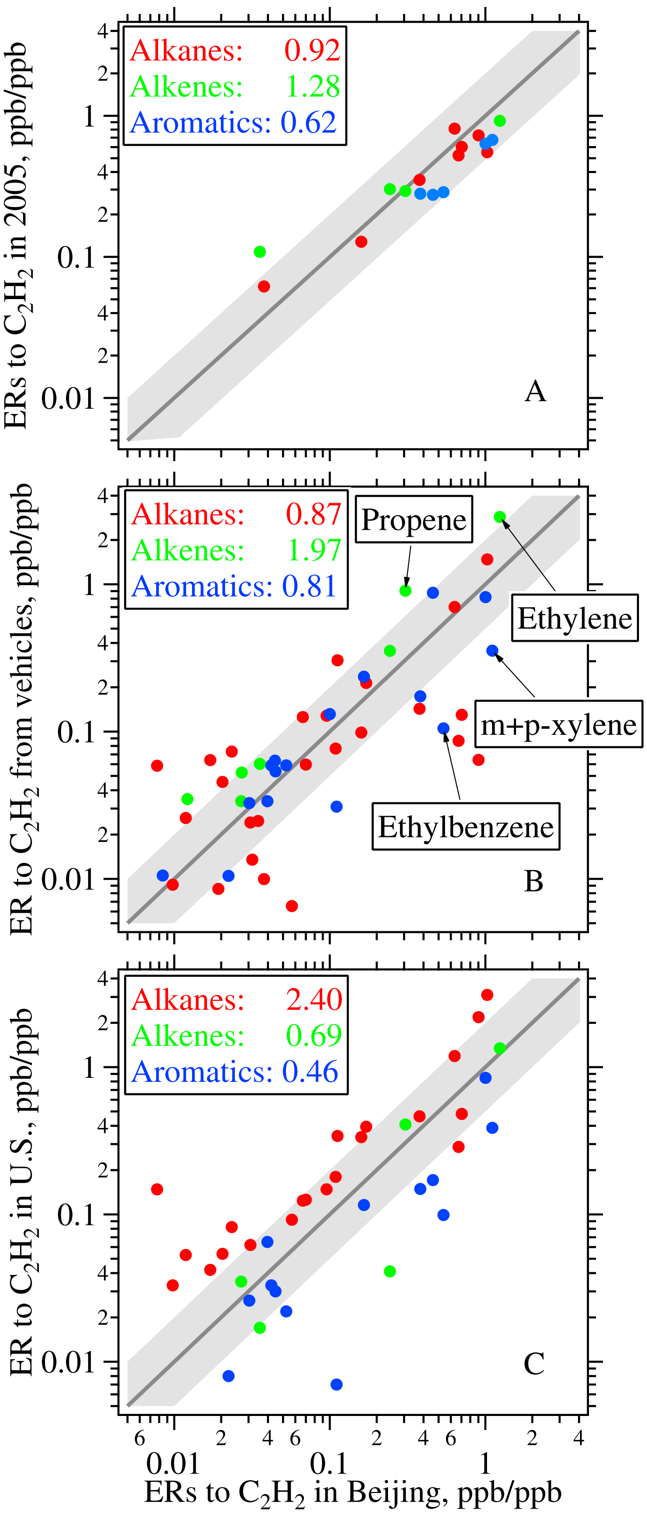

Figure 4. Comparisons of emission ratios of hydrocarbons to C_2H_2 in 2010 of Beijing with those from the measurements in 2005 (a) of Beijing, (b) in exhausts of gasoline-powered vehicles [*Liu et al.*, 2008], and (C) in northeastern United States [*Warneke et al.*, 2007]. The numbers in the legend are the geometric means of the ratios of *y* axis values to *x* axis values for each class of hydrocarbons [*Parrish et al.*, 1998]. The black lines indicate the 1:1 relationship, and the gray areas show agreements within a factor of two.

[22] Besides the 2010 measurement, a NOAA GC-MS/FID was deployed at the same site in August 2005 to measure a series of hydrocarbons and OVOCs. Detailed information about the 2005 measurements can be found in previous papers [*Y. Liu et al.*, 2009; *Shao et al.*, 2009]. The same procedure for calculating emission ratios of hydrocarbons was also applied to the 2005 measurements and the results are also shown in Table 1. Figure 4a compares the emission ratios of hydrocarbons determined in 2005 and 2010. Hydrocarbons were divided into three different groups: alkanes, alkenes and aromatics. Geometric mean (see further discussions about geometric mean in *Parrish et al.* [1998]) of the ratios of the emission ratios determined in the two different years for each group of hydrocarbons is calculated and shown in Figure 4. Generally, emission ratios of most VOCs species in the 2 years agreed within a factor of two as indicated in the shaded areas. Though emission ratios of aromatic species in 2005 were lower than the values in 2010, the differences were lower than the combined uncertainties of the determination of the emission ratios. Thus, the evidence suggests that VOCs emission compositions in Beijing were similar in 2005 and 2010.

[23] The emission ratios in Beijing were also compared with the previous reported emission profile of gasoline-powered vehicles in China [*Liu et al.*, 2008], as shown in Figure 4b. Good agreement was obtained for most hydrocarbons, with the exception of ethylene, propene and C8 aromatics (ethylbenzene, xylenes and styrene). The agreement indicates that the emissions of gasoline-powered vehicles are the main source of VOCs in Beijing, which is consistent with the results in previous studies [*Shao et al.*, 2009]. The emission ratios of hydrocarbons to acetylene determined in Beijing can also be compared with those obtained in northeastern U.S. [*Warneke et al.*, 2007], as illustrated in Figure 4c. Our calculated emission ratios in Beijing agreed well with those in northeastern U.S. for many hydrocarbons. However, two main discrepancies were observed in the comparison: emission ratios of some alkanes (ethane, propane and C6–C8 branched alkanes) are lower in Beijing and emission ratios of C8 aromatics in Beijing are significantly higher. Interestingly, it was shown that emission ratios of many alkanes determined in northeastern U.S. are higher than those in vehicle exhausts, which was attributed to significant contributions from area sources, especially light alkanes [*Warneke et al.*, 2007]. The higher C8 aromatics in Beijing compared to emissions of gasoline-powered vehicles and those in northeastern U.S. may be due to the contribution of industrial emissions and/or solvent use in Beijing, as a result of the rapid construction activities in Beijing and its surrounding areas. Source profiles of solvent use in Beijing showed that C8 aromatics are the main components of VOCs [*Yuan et al.*, 2010]. On the other hand, the differences of VOCs emission between the two regions in China and U.S. could also possibly be caused by different fuel compositions, different fleet ages and different emission control technologies for vehicles.

[24] CO has proven to be a good tracer for urban emissions [*de Gouw et al.*, 2008] and many literature studies have reported emission ratios of VOCs to CO in the literatures [*von Schneidemesser et al.*, 2010; *Warneke et al.*, 2007]. In this study, VOCs/CO emission ratios are not calculated directly based on the parameterization method above. The reasons for this are (1) the data coverage for CO during the

Table 2. Parameters Describing OVOC Concentrations in Beijing

Species	ER_{OVOC} (ppb [ppb C_2H_2]$^{-1}$)	$ER_{precursor}$ (ppb [ppb C_2H_2]$^{-1}$)	k_{ovoc}[a] (10^{-12} cm^3 molecule^{-1} s^{-1})	$k_{precursor}$ (10^{-12} cm^3 molecule^{-1} s^{-1})	$ER_{biogenic}$ (ppb [ppb isoprene]$^{-1}$)	Background (ppb)
Formaldehyde	0.72 ± 0.11	6.40	9.4	2.87	0.98 ± 0.07	0.94 ± 0.21
Acetaldehyde	0.72 ± 0.05	3.45	15	2.41	0.17 ± 0.03	0.29 ± 0.10
Propanal[b]	0.02 ± 0.02	2.04	20	2.45	0.14 ± 0.01	0.31 ± 0.03
n-Butanal[b]	0.002 ± 0.005	1.66	24	0.58	0.04 ± 0.00	0.10 ± 0.01
Acetone	0.57 ± 0.05	1.47	0.17	1.05	0.18 ± 0.03	1.98 ± 0.09
MEK	0.31 ± 0.01	0[c]	1.22	0[c]	0.07 ± 0.01	0.06 ± 0.04
Methanol	3.43 ± 0.11	0[c]	0.94	0[c]	0.02 ± 0.11	5.76 ± 0.37

[a] The rate coefficients of OVOC (k_{OVOC}) are from *Atkinson and Arey* [2003a] and *Atkinson et al.* [2006].

[b] Propanal and n-butanal data are from GC-MS/FID, and other species are from PTR-MS.

[c] The fitting values are negative. These parameters are set to zero and the fit is repeated.

campaign was not as good as for acetylene, and (2) estimation of CO background concentration introduces extra uncertainties [*Warneke et al.*, 2007]. Instead, we calculated VOCs emission ratios to CO from emissions ratios to acetylene in Table 1 and emission ratio of acetylene/CO. The lifetimes of acetylene and CO in the atmosphere are both on the order of several weeks. The emission ratio of acetylene to CO is determined from the slope of the correlation between these two compounds (not shown). The correlation was strong (R = 0.82) with a slope of 3.92 ± 0.13 ppb/ppm. The value is consistent with the ratios reported for Beijing in 2005 and other mega-cities in the world [*Parrish et al.*, 2009]. The calculated emission ratios of hydrocarbons to CO are also tabulated in Table 1.

3.2.3. Sources and Chemistry of OVOCs

[25] There are both primary emissions and secondary formation for OVOCs. Some OVOCs can also be emitted by plants or oxidized from other biogenic compounds (e.g., isoprene). Following the method developed by *de Gouw et al.* [2005], OVOCs concentrations are divided into four parts: anthropogenic primary emissions, anthropogenic secondary formations, biogenic sources and background.

$$\begin{aligned}[\mathrm{OVOC}] = {} & \mathrm{ER_{OVOC}} \times [\mathrm{C_2H_2}] \times \exp(-(k_{\mathrm{OVOC}} - k_{\mathrm{C_2H_2}})[\mathrm{OH}]\Delta t) \\ & + \mathrm{ER_{precursor}} \times [\mathrm{C_2H_2}] \times \frac{k_{\mathrm{precursor}}}{k_{\mathrm{OVOC}} - k_{\mathrm{precursor}}} \\ & \times \frac{\exp(-k_{\mathrm{precursor}}[\mathrm{OH}]\Delta t) - \exp(-k_{\mathrm{OVOC}}[\mathrm{OH}]\Delta t)}{\exp(-k_{\mathrm{C_2H_2}}[\mathrm{OH}]\Delta t)} \\ & + \mathrm{ER_{biogenic}} \times \mathrm{Isoprene_{source}} + [\mathrm{bg}] \qquad (3)\end{aligned}$$

where [OVOC], [C_2H_2] and [bg] are concentrations of measured OVOCs, acetylene and OVOCs background concentrations, respectively. ER_{OVOC} and $ER_{precursor}$ are emissions ratios of OVOCs and OVOCs precursors relative to acetylene. [OH]Δt is calculated from equation (1). $k_{C_2H_2}$, k_{OVOC} and $k_{precursor}$ are OH rate constants of C_2H_2, OVOCs species and OVOCs precursors, respectively. $ER_{biogenic}$ is the emission ratios of OVOCs to isoprene source concentrations ($Isoprene_{source}$) from biogenic emissions. $Isoprene_{source}$ is calculated from concentrations of isoprene and its photochemical products MVK and MACR [*Apel et al.*, 2002; *de Gouw et al.*, 2005; *Stroud et al.*, 2001]. In equation (3), the parameters of ER_{OVOC}, $ER_{precursor}$, $k_{precursor}$, $ER_{biogenic}$ and [bg] are unknown and they are estimated from least squares fits.

[26] The fit results for formaldehyde are shown in Figure 3. The stacked concentrations from the four parts in equation (3) compared well with measured concentrations, with a correlation coefficient of 0.80. From the fit, a background level of 0.94 ± 0.21 ppb for formaldehyde was obtained, contributing 15% of formaldehyde concentrations in the whole campaign. Anthropogenic primary emissions, anthropogenic secondary formation and biogenic sources accounted for 22%, 28% and 35% of formaldehyde concentrations, respectively. The parameter of $ER_{biogenic}$ was calculated to be 0.98 ± 0.07 ppb [ppb isoprene]$^{-1}$. Using the formaldehyde yield from isoprene oxidation (0.57–0.63) [*Atkinson and Arey*, 2003b], the contributions of isoprene oxidation to formaldehyde formation was estimated at 20–22%. Previously, *Pang et al.* [2009] reported that isoprene oxidation accounted for 4.6–11.5% of formaldehyde concentrations in Beijing (March–November), with a maximum in August when our campaign took place. The value from *Pang et al.* [2009] was somewhat lower than our estimate, which may be due to different measurement locations and the omission of MVK and MACR reactions with OH radicals in Pang's study.

[27] Fits similar to that for formaldehyde were also done for other OVOCs species measured in the campaign. The fitting parameters and the allocated fractions to the four parts are shown in Table 2 and Table 3, respectively. The correlation coefficients between measured and calculated concentrations were also high for other OVOCs species, ranging from 0.74 to 0.84. In general, the contributions from anthropogenic secondary formation are more important for aldehydes (26–36%) than ketones and alcohols (0–5%). It should be mentioned that secondary formations for MEK and methanol were not observed in this study. Biogenic sources accounted for 0–36% of the OVOCs concentrations. Previous evidence indicated that biogenic emissions are important contributors to ozone formation at the present measurement site, merely considering

Table 3. Correlation Coefficients of Measured and Calculated OVOC Concentrations and the Contribution Fractions From Different Sources to OVOC Concentrations

Species	R	Primary Anthropogenic (%)	Secondary Anthropogenic (%)	Biogenic (%)	Background (%)
Formaldehyde	0.80	22	28	36	15
Acetaldehyde	0.78	46	30	16	8
Propanal	0.77	3	36	31	30
n-Butanal	0.74	1	26	36	37
Acetone	0.80	38	5	9	47
MEK	0.84	80	0	14	6
Methanol	0.84	62	0	0	38

contribution from isoprene [*Lu et al.*, 2010; *Xie et al.*, 2008]. Thus, if the contributions of biogenic sources to OVOCs, especially the highly reactive aldehydes, were included in the evaluation, the role of biogenic emissions in ozone formation would be more significant. As shown in Figure 3, the concentrations of various VOCs reached the lowest concentration in the campaign on 14 August, 12:00 P.M.-24:00 P.M., when the prevailing wind was from northern China and Mongolia where both anthropogenic and biogenic emissions are lower. The background terms of various OVOCs species from the fits were generally close to the minimum concentrations measured on 14 August. Thus, background concentrations tabulated in Table 2 should be interpreted as regional backgrounds in northern China.

[28] It is interesting to compare the allocation results of OVOCs between Beijing and northeastern U.S. during the NEAQS 2002 campaign [*de Gouw et al.*, 2005]. Though emission ratios of acetaldehyde to acetylene were are comparable in Beijing (0.72 ± 0.07 ppb/ppb) and northeastern U.S. (0.83 ± 0.07 ppb/ppb), the fraction from anthropogenic primary emissions for acetaldehyde in Beijing (46%) was significantly larger than those in the northeastern U.S. (9%). The determined $[OH]\Delta t$ were in the range of $0–5.4 \times 10^{11}$ cm^{-3} s in the NEAQS 2002 campaign, whereas $[OH]\Delta t$ varied among $0–1.2 \times 10^{11}$ cm^{-3} s in Beijing campaign, with an average of 4.9×10^{10} cm^{-3} s. Thus, the air measured at the urban Beijing site had experienced less aging processes than that in NEAQS 2002 campaign, where the measurement were made aboard ship offshore from the urban areas. Acetaldehyde concentrations from primary emissions decrease exponentially similar to NMHCs species. As a consequence, more acetaldehyde concentrations from anthropogenic primary emissions remained in the atmosphere during the Beijing campaign and the primary fraction was more important than that during the NEAQS 2002 campaign. Other OVOCs species (e.g., acetone) also showed larger percentages from anthropogenic primary emissions in Beijing than that in the northeastern U.S. In general, the different times of aging in the atmosphere can explain the differences of OVOCs allocation results between the Beijing and NEAQS 2002 studies.

3.3. Results From PMF Analysis

3.3.1. Determination of PMF Factor Number

[29] PMF was applied to the measured VOCs data set, by using PMF2 in robust mode [*Paatero*, 1997] and evaluating the results in the PMF Evaluation Tools (PET) recently developed by *Ulbrich et al.* [2009]. Hydrocarbons species measured by online GC-MS/FID (N = 54) and masses from PTR-MS (N = 19) were combined into a unified data set. The OVOCs species measured from GC-MS/FID was not included in the PMF and most of information from these OVOCs species can be represented by the masses from PTR-MS. Only the periods with measured data points from both of the two instruments were included in the PMF analysis. In total, the data matrix for PMF was composed by 464 rows (samples) × 73 columns (species per sample).

[30] The uncertainties of NMHCs concentrations determined by GC-MS/FID were calculated as the sum of 10% of concentrations and 1/3 of detection limits. The uncertainties of PTR-MS masses were are calculated as the sum of 10% of measured concentrations and the errors from signal sampling of ions by mass spectrometer, which are estimated by counting statistics of VOCs masses [*de Gouw and Warneke*, 2007; *de Gouw et al.*, 2003]. The method recommended by *Hopke* [2000] was followed to determine the concentrations and uncertainty values for missing data points and those below detection limit. The concentrations of missing data points were replaced by the median concentrations and the uncertainties were set to 4 times of the median concentrations. For below detection limit values, the concentrations were set as half of the detection limit and the uncertainties were set to 5/6 of the detection limits. All of the compounds have signal-to-noise ratios (SNR) larger than two in this study.

[31] PMF factor numbers were explored from 1 to 6 for the best solution. For each factor number, different random starting points (SEEDs = 1–10) were tried to find the local minimum in the PMF solutions [*Paatero*, 1997]. The rotation ambiguity was explored by varying the fPeak values from −3 to 3. In this study, results from nonzero fPeak values are generally consistent with the runs associated with zero fPeak values (fPeak = 0). The results shown below are associated to no rotation in the PMF analysis. The weighting of the data from two instruments (GC-MS/FID and PTR-MS) in PMF should not significantly influence the following conclusions, as inferred from the even number of negative and positive residual values of the both instruments in rows of the matrix [*Slowik et al.*, 2010] and the results from PMF runs using individual data sets in section 4.3. Bootstrap analyses were run for 100 times to calculate the uncertainties of PMF results [*Norris et al.*, 2008]. The Q/Q_{exp} values and mass fractions of the factors in the PMF solutions from 1 to 6 are shown in Figure 5. It is expected that additional factors in PMF decrease Q/Q_{exp} gradually. There is a large decrease of Q/Q_{exp} from 1 factor to 2 factors (26%) and from 3 factors to 4 factors (19%). When the factor number is 4, Q/Q_{exp} was 2.9. As the size of factor continues to increase up to 5 or larger, the change of Q/Q_{exp} is not strong (lower than 10% in *Ulbrich et al.* [2009]).

[32] Time series of the factors in the two-factor solution correlated well with NO_x and PAN, respectively. The two factors are regarded as a primary factor and a secondary +transport factor. Two different solutions were observed as the factor number increased to 3. One solution associated with most of the tested random seeds (except SEED = 3) resolved three anthropogenic factors, which correlated well with NO_x, CO and O_x ($=O_3 + NO_2$), respectively. The other solution (SEED = 3) extracted two factors similar to the two-factor solution and an extra biogenic factor with time series analogous to isoprene. The four-factor solution combined the two situations of the three-factor solutions, with three anthropogenic factors and a biogenic factor. As more factors were added into PMF, time series or profiles of the newly resolved factors correlated well with those of the already-existing factors. Thus, the four-factor solution was chosen as the best solution from PMF.

3.3.2. Time Series and Profile of PMF Factors

[33] Time series, diurnal variations and profiles of the resolved factors in the four-factor solution are shown in Figure 6, Figure 7 and Figure 8, respectively. As discussed above, the first factor correlated well with CO with a correlation coefficient of 0.82. It had no distinct diurnal variation and the main species in the profile were low-weight alkanes, ethylene, acetylene, benzene, toluene, methanol and some other oxygenates. The second factor had a maximum

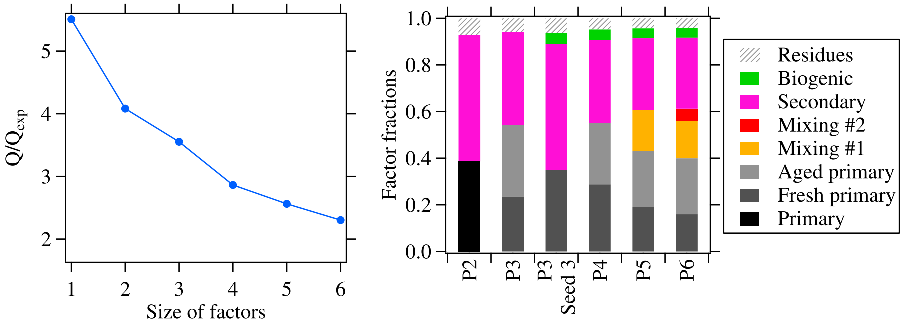

Figure 5. (left) Q/Qexp values as a function of factor number in PMF; (right) mass fractions from various factors in different PMF solutions.

concentration in the midday. It was regarded as a biogenic factor, because isoprene and oxygenates were large contributors to the profile. Time series of the third factor followed well with NO_x (R = 0.80), with high concentrations at night and low in the daytime. All of the main compounds in the profile of factor 1 were observed in that of factor 3, but the abundances of the high-reactive species (e.g., C8–C9 aromatics) were larger in factor 3. In the view of the different reactivities of CO and NO_x, factor 1 and factor 3 were termed as aged primary factor and fresh primary factor, respectively. Time series of the fourth factor followed well with secondary formed tracers (O_x, R = 0.63; PAN, R = 0.79). Diurnal cycles of the fourth factor showed a maximum concentration in the afternoon and evening. The fourth factor was named as secondary+transport factor.

[34] The reconstructed concentrations of propane, 1,2,4-trimethylbenzene and formaldehyde from PMF are shown in Figure 9. The reconstructed concentrations compared well with the measured concentrations for all three compounds and the correlation coefficients were 0.92, 0.97 and 0.95, respectively. Propane was mainly contributed from the aged primary factor (49%), whereas fresh primary factor accounted for the major percentages of 1,2,4-trimethylbenzene (74%). As one of the most abundant OVOCs, formaldehyde is mainly contributed by the secondary+transport factor (68%).

[35] It is interesting to compare the quality of the fits between the photochemical age parameterization method and PMF. The correlation coefficients (R) of calculated concentrations with measured concentrations for the three compounds by the photochemical age-based parameterization method are 0.81, 0.84 and 0.77, respectively, i.e., significantly lower than the values from PMF. Correlation coefficients of measured and calculated concentrations of various hydrocarbons from the parameterization method average 13% lower than the results in PMF. It may be more appropriate to compare the correlation coefficients from the parameterization method with those in the two-factor solution of PMF analysis, since only two parameters (acetylene and OH exposure) were used to model the concentrations of hydrocarbons in the parameterization method. However,

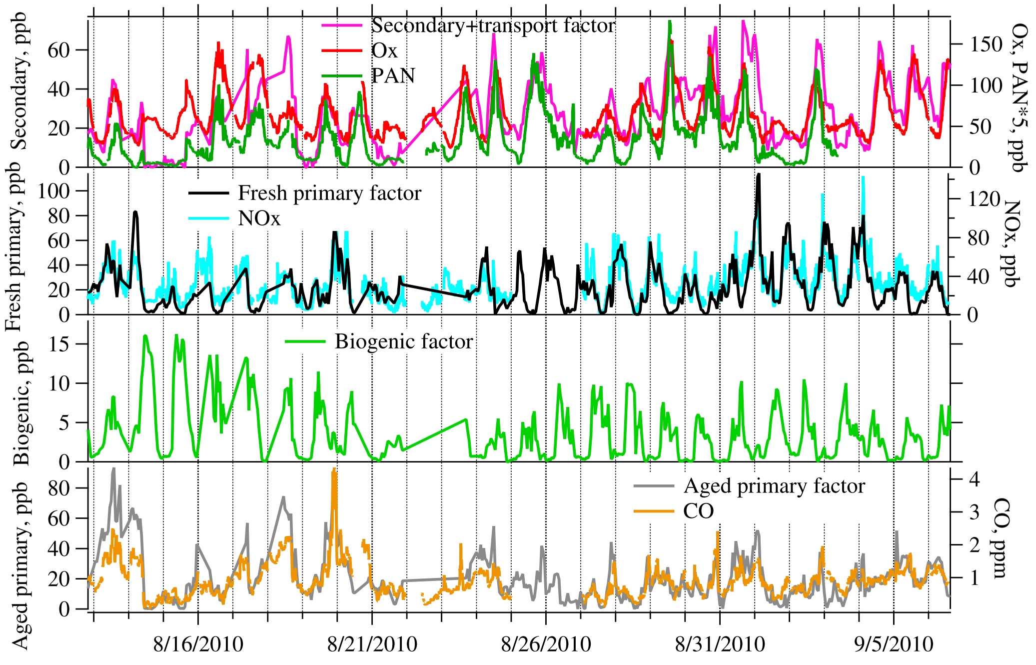

Figure 6. Time series of the resolved factors from the PMF. Time series of tracers are also shown in the graphs for comparisons, including CO, NO_x, O_x (=NO_2 + O_3) and PAN.

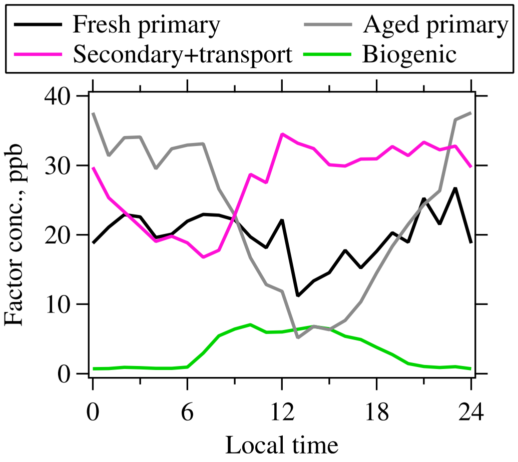

Figure 7. Diurnal variations of the resolved factors from the PMF.

correlation coefficients in the two-factor solution of PMF are also significantly higher (10%) than in the parameterization method. The results indicate that PMF generally explained more variability of VOCs concentrations than the photochemical age-based parameterization method for the VOCs data set measured in Beijing.

4. Discussions

4.1. Exploring the Meaning of Anthropogenic Factors

[36] In this study, the three anthropogenic factors extracted from PMF are not termed as individual sources (e.g., vehicle emissions, solvent usage or gasoline evaporation). In previous studies, such assignments have been usually based on abundances of VOCs species or ratios of VOCs pairs in the PMF profiles. An attempt was made to assign the factors to specific sources using the methods in the literature. Taking gasoline evaporation as an example, many studies used i/n-pentane as the indicators for this source [*Buzcu and Fraser*, 2006; *Song et al.*, 2007]. However, here these two compounds were observed in all three anthropogenic factors, as were rich abundances of oxygenated VOCs (such as aldehydes and ketones), which are not usually observed in the gasoline [*Harley et al.*, 2000]. Assigning a single factor as gasoline evaporation was not possible. Thus, exploring the physical meanings of the resolved PMF factors is essential in this study and it is discussed in the following parts.

[37] The contributions of the resolved PMF factors to each NMHCs species were calculated. Figure 10 shows the scatterplots of factor contributions to each NMHCs species as a function of its OH rate constant (k_{OH}) [*Atkinson et al.*, 2006]. It should be noted that the blue lines in Figure 10, which are the polynomial fits to the data point, are drawn to guide eyes. If a factor extracted from PMF originates from a specific VOCs source, then no dependence is expected in Figure 10. The biogenic factor does show this expected behavior, as shown in Figure 10. However, this is not the case for the three anthropogenic factors. Factor fractions of the fresh primary factor increased as VOCs became more reactive. Opposite trends are observed for the aged primary factor and the secondary +transport factor. The aged primary factor and the secondary +transport factor were the main contributors to relatively unreactive species (e.g., acetylene and benzene), whereas the fresh primary factor accounted for the major fractions of highly reactive species (e.g., 1,2,4-trimethylbenzene). This behavior suggests that the separation of factor contributions to NMHCs species among the three anthropogenic factors is not perfect. The allocation of the VOCs concentrations to the three anthropogenic factors depended on their k_{OH} values. The contributions of fresh and aged primary factors to some C8–

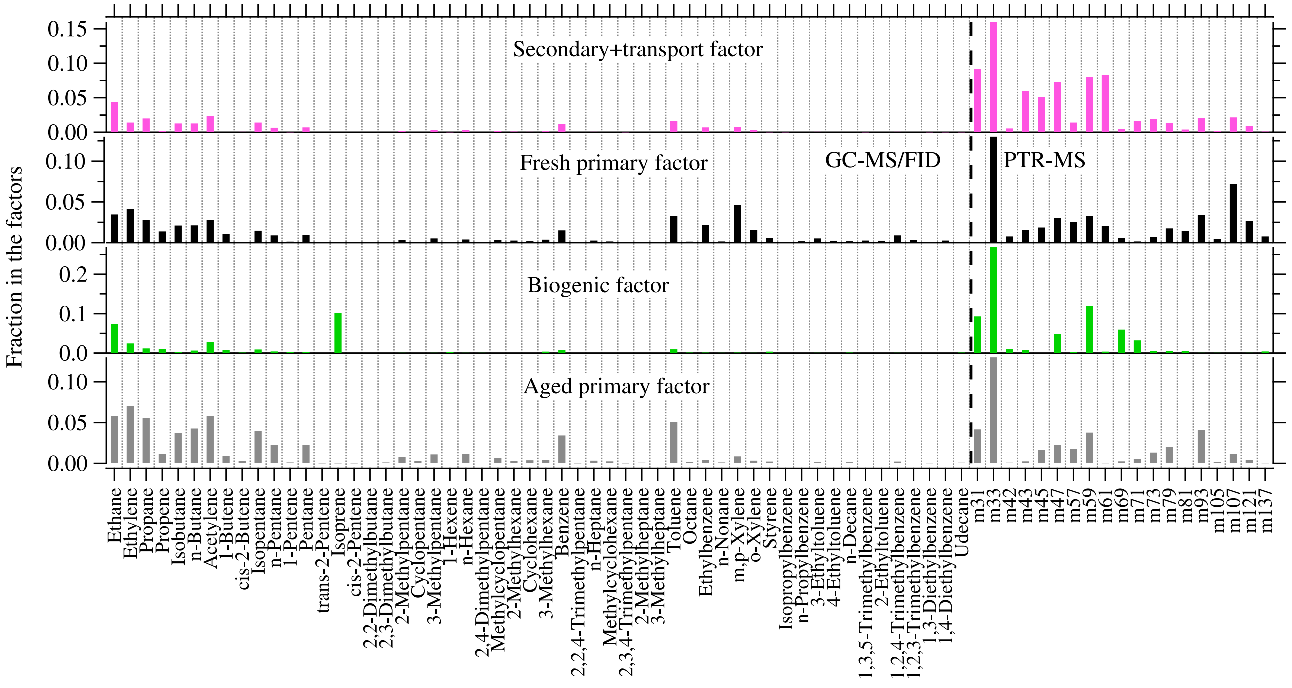

Figure 8. Profiles of the resolved factors from the PMF.

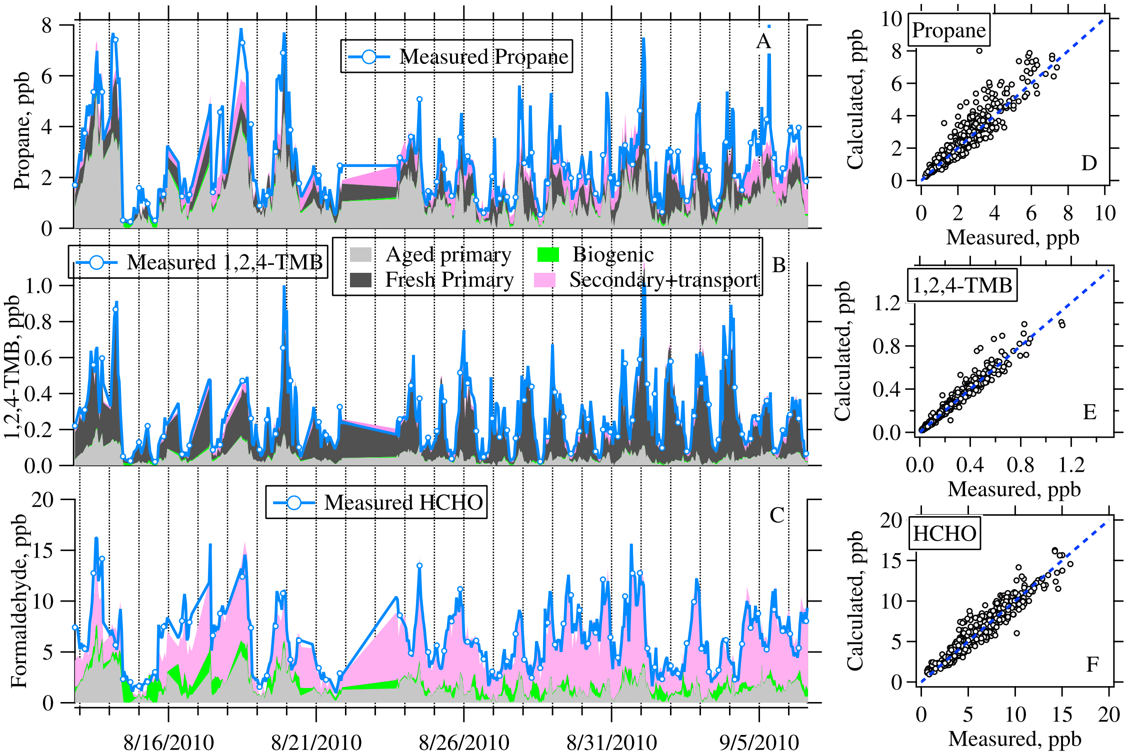

Figure 9. Comparisons of VOCs concentrations between measured and calculated from the PMF for (a) propane, (b) 1,2,4-TMB, and (c) formaldehyde. Scatterplots of the calculated and measured concentrations for (d) propane, (e) 1,2,4-TMB, and (f) formaldehyde. The blue dashed lines are the 1:1 relationship.

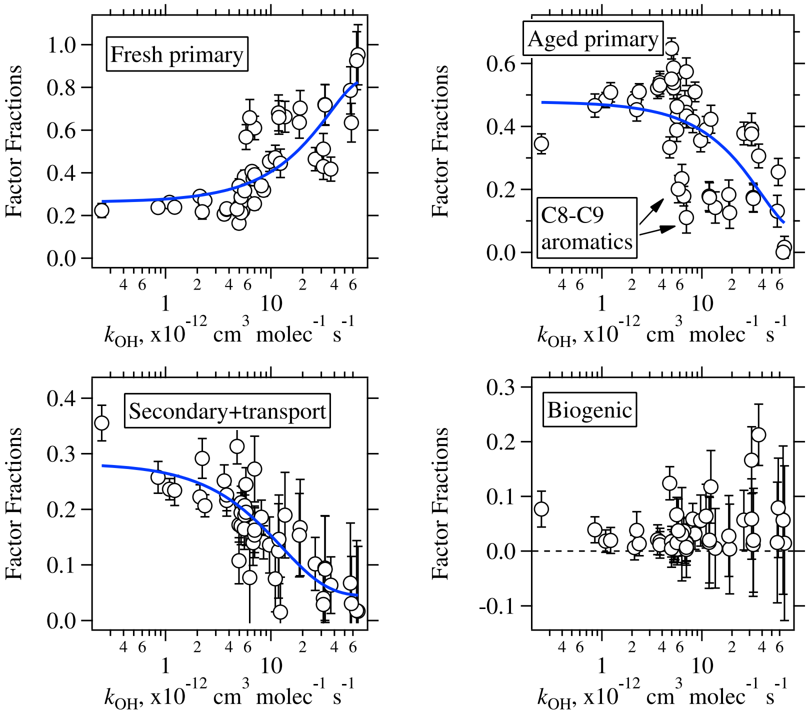

Figure 10. Factors contributions to each NMHC species as a function of its k_{OH} value. Each data point represents one compound. Error bars indicate standard deviations from bootstrap runs. Blue lines are the polynomial fit lines to the data points to guide eyes.

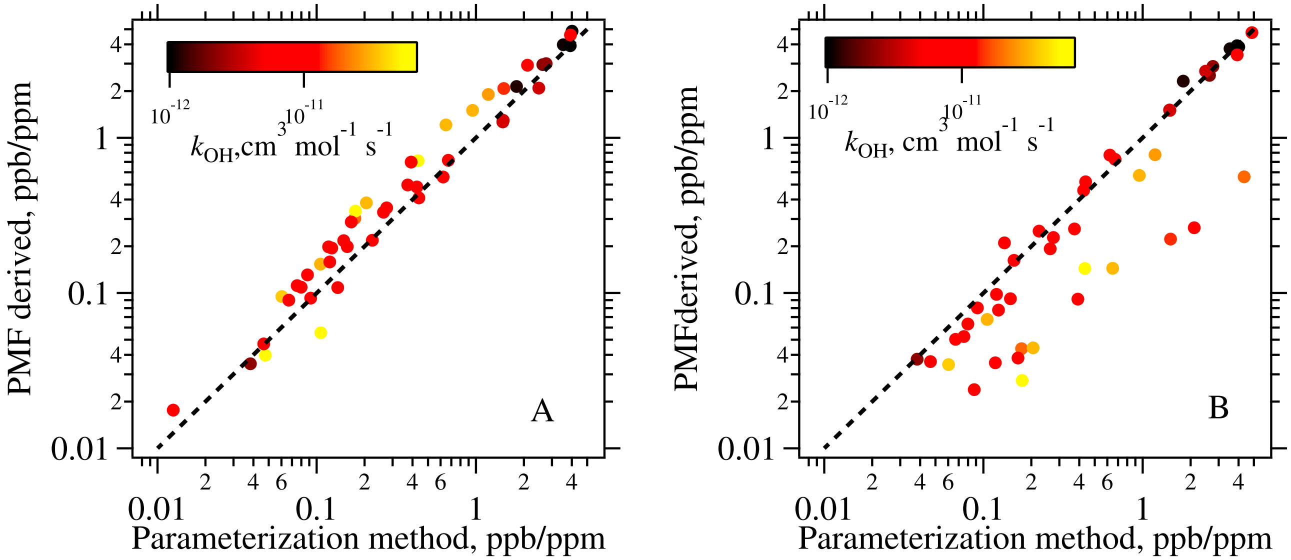

Figure 11. Comparison of emission ratios of NMHCs to CO from PMF with the photochemical age-based parameterization method: (a) fresh primary factor and (b) aged primary factor. Data points are color-coded by k_{OH} value of each VOC species. The dashed lines indicate the 1:1 relationship.

C9 aromatics deviate a little from the corresponding dependence lines, which may be due to the emissions of these compounds from specific sources (e.g., solvent use).

[38] Factor profiles provide additional insight into the physical meaning of the PMF factors. Factor profiles represent the relative abundances of VOCs compounds in the factors; thus emission ratios of VOCs species to CO can be calculated from the profiles:

$$ER_i = \frac{\mathrm{Profile}_i \times ER_{C_2H_2}}{\mathrm{Profile}_{C_2H_2}} \quad (4)$$

where ER_i and $ER_{C_2H_2}$ are emission ratios of VOCs species relative to CO and emission ratios of acetylene to CO, respectively. $ER_{C_2H_2}$ is derived from the slope in the scatterplot of C_2H_2 with CO (3.92 ± 0.13 ppb/ppm) (see section 3.2). $\mathrm{Profile}_i$ and $\mathrm{Profile}_{C_2H_2}$ are the abundances of VOCs species and acetylene in the profile of a specific factor.

[39] The NMHCs emission ratios determined from PMF factor profiles can be compared to the emission ratios obtained from the photochemical age-based parameterization method of section 3.2. Emission ratios calculated from the fresh primary factor profile (Figure 11a) agreed well with the parameterization method (slope = 1.12, R = 0.99), with no distinct dependence upon k_{OH} values. This agreement indicates that the fresh primary factor does indeed represent VOCs signatures from urban emissions with no photochemical processing. In contrast, the aged primary factor profile significantly underestimated emission ratios of highly reactive NMHCs species (Figure 11b), although there is good agreements for inert NMHCs species. The calculation for the profile of the secondary+transport factor gave results similar to the aged primary factor (not shown). These results indicate that the aged primary factor and secondary+transport factor represented air masses that were more photochemically aged relative to the fresh primary factor.

[40] The relationship between two anthropogenic factors can be further explored by comparing the factor profiles. If one factor is photochemically derived from another factor, the ratios of VOCs abundances in $\mathrm{Profile}_i$ and $\mathrm{Profile}_j$ ($R_{\mathrm{profile}_i/\mathrm{profile}_j}$) should follow this equation:

$$R_{\mathrm{profile}_i/\mathrm{profile}_j} = A \times \exp(-k_{OH} \times [OH]\Delta t). \quad (5)$$

[41] Here, A is a scaling factor, which accounts for the normalization procedures in PMF profiles that make the VOCs abundances sum to unity. Equation (5) is adapted from the concentration ratios equation in *Kleinman et al.* [2003] (equation (1) in the reference), which was used to calculated photochemical ages in Phoenix.

[42] Figure 12 shows the dependence of $R_{\mathrm{aged\ primary/fresh\ primary}}$ and $R_{\mathrm{secondary+transport/fresh\ primary}}$ upon k_{OH}. Anticorrelations are observed for both pairs of profiles. Blue lines show fits of equation (5) to the data. The values of OH exposure ($[OH]\Delta t$) are estimated as 8.1×10^{10} molecule cm^{-3} s and 1.4×10^{11} molecule cm^{-3} s from the two fits. The two OH exposure values represent the differences of photochemical processing between the factors in each pair (aged primary/fresh primary, secondary+transport/fresh primary). The ability of equation (5) to reproduce these relationships indicates that the aged primary factor and secondary+transport factor were both derived from the fresh primary factor by photochemically processing. Thus, the three anthropogenic factors from PMF are not independent; i.e., they were interrelated by photochemical processing in the atmosphere.

4.2. Separation of Anthropogenic and Biogenic Contributions in PMF

[43] A biogenic factor with high fractions of isoprene was resolved from the PMF analysis. The abundances of isoprene and MVK+MACR were respective 10.3% and 3.2%, resulting in an MVK+MACR/isoprene ratio of 0.31. According to the isoprene chemistry described in section 3.2, this ratio corresponds to photochemical processing time for this

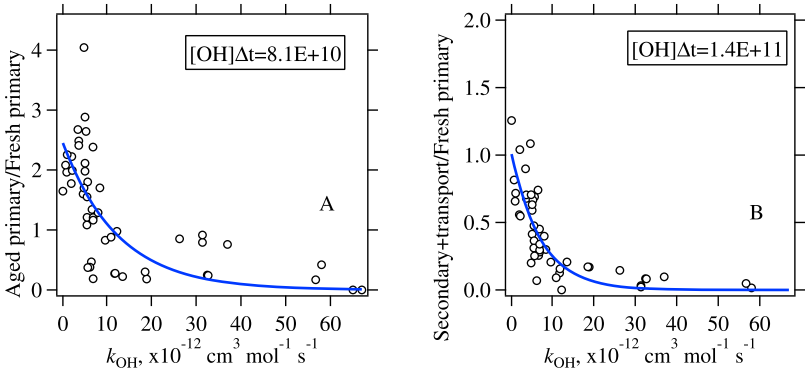

Figure 12. Abundance ratios of NMHCs from two profiles as a function of hydrocarbon k_{OH} values: (a) aged primary factor/fresh primary factor and (b) secondary+transport factor/fresh primary factor. The blue lines are the fit results from equation (5).

biogenic factor of only about 17 min (assuming daytime average OH concentration was 4.5 × 10^6 molecule cm^{-3}) [*Lu et al.*, 2012]. The correlation of MVK+MACR with isoprene during the whole campaign is shown in Figure 13. The ratio of MVK+MACR to isoprene from biogenic factor (0.31) lies in the lower edge of the measured ratios in the atmosphere. Consequently, the biogenic factor in PMF can only be interpreted as the most freshly emitted biogenic emissions intercepted at the measurement site. However, the contribution of the biogenic factor to MVK+MACR concentrations in the whole campaign was only 16% and the majority of MVK+MACR concentrations (65%) were from the secondary+transport factor. The ratio of MVK+MACR to isoprene in the secondary+transport factor (84.7) lies in the higher edge of the measured concentration ratios (Figure 13). Since MVK and MACR are the oxidation products of isoprene, this relationship indicates that a large fraction of secondary biogenic VOCs fell into the secondary+transport factor. Diurnal profiles of MVK and MACR (Figure 1) had a pattern similar to the secondary+transport factor. Since oxidation of isoprene and anthropogenic VOCs occurs simultaneously, it is not surprising that PMF includes OVOC products of both VOCs classes in the secondary+transport factor.

[44] In addition to isoprene and MVK+MACR, methanol, formaldehyde, acetone and ethane were also elevated in the profile of the biogenic factor (Figure 8). It is not surprising that oxygenates are high in biogenic emissions [*Guenther*, 2002]. But, the high abundance of ethane in biogenic profile (7.3%) and the contribution of biogenic factor to ethane concentration (7.7%) are unexpected, since biogenic emission is not a significant source of ethane [*Xiao et al.*, 2008]. As shown in Figure 10, the biogenic factor also accounted for nonnegligible contributions to many other nonisoprene hydrocarbons. On average, the biogenic factor contributed 3% of the total concentrations of these hydrocarbons measured by GC-MS/FID. The total abundance of hydrocarbons in the profile of biogenic factor was 23%, twice the isoprene abundance (10.3%) in the profile. Among these hydrocarbons, only some alkenes (e.g., ethylene, propene and 1-butene) are showed to be emitted at significant rates by plants [*Goldstein et al.*, 1996]. Assuming that there was no biogenic emission of these hydrocarbons, the biogenic factor would overestimate biogenic emissions by 30% at most.

[45] As discussed above, biogenic emissions and anthropogenic emissions were not separated completely in the PMF. The secondary+transport factor contained concentrations of oxidation products from biogenic emissions, whereas the biogenic factor accounted for a fraction of anthropogenic hydrocarbon concentrations. Thus, using the results from PMF to evaluate the importance of biogenic emissions in the urban environment (e.g., Beijing) also has some limitations.

4.3. Further Analysis of Other PMF Solutions and Results of Individual Data Sets

[46] Besides the four-factor solution discussed above in detail, the analyses of the physical meaning of PMF factors presented in sections 4.2 and 4.3 were also applied to the factors in other PMF solutions with different factor numbers. The relative contributions of the anthropogenic factors to each hydrocarbon in two-factor solution and three-factor solutions showed similar dependence upon its k_{OH} values. Though fractions of the newly resolved factors illustrated no distinct dependence on k_{OH} values of hydrocarbons as the factor number increases to 5 and 6, other already-existing

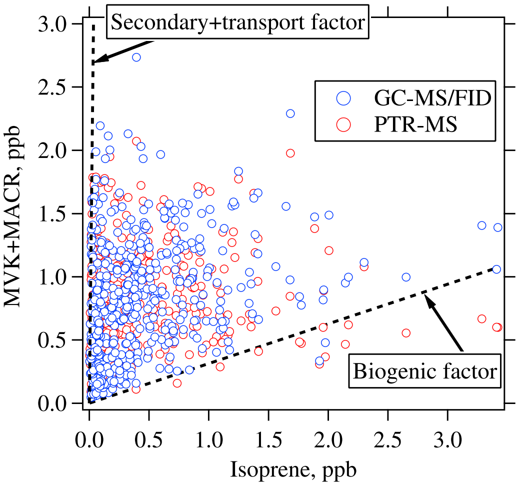

Figure 13. Correlations of MVK+MACR with isoprene. The dashed lines show the ratios of (MVK+MACR)/isoprene in biogenic factor and secondary+transport factor in PMF, respectively.

anthropogenic factors still contributed the majority of VOCs concentrations (Figure 5). In the solutions with a biogenic factor resolved, the concentrations of isoprene and MVK +MACR were still mainly contributed by the biogenic and the secondary+transport factor, respectively, suggesting that all of the biogenic factors only represented fresh biogenic emissions. These results suggest that the PMF results in other solutions were also strongly influenced by photochemical processing.

[47] In most of previous studies, only NMHCs species were incorporated in PMF. To explore the effects of VOCs species in the model to PMF results, PMF was run separately on the data measured by GC-MS/FID and PTR-MS, respectively. The evaluation methods for these PMF results were identical to the combined data set. PMF extracted three factors (fresh primary factor, aged primary factor and biogenic factor) and four factors from GC-MS/FID data set and PTR-MS data set, respectively. The secondary+transport factor was not resolved from GC-MS/FID data set, since no OVOCs species was included in the data set. Both time series and profiles of these resolved factors agreed well with those of the respective factors from the combined data set ($R > 0.95$). This agreement leads to two main conclusions: (1) consistent results were obtained from the PMF analyses of the combined data set and individual data sets, and (2) factors in PMF from different data sets were extracted according to different degree of photochemical processing, not just based on the individual sources.

5. Conclusions

[48] We measured volatile organic compounds (VOCs) at an urban site in Beijing in August–September 2010. A photochemical age-based parameterization method was applied to characterize VOCs chemistry in the atmosphere and to extract relative emissions of VOCs. This method assumes that two emissions sources, anthropogenic and biogenic, combined with photochemical aging are responsible for VOCs concentrations at the ground site. Most of the variability in both NMHCs and OVOCs concentrations is explained by the parameterization method. The emission ratios of hydrocarbons determined in Beijing agreed within a factor of two between data sets collected in 2005 and 2010. Emission ratios of some alkanes are significantly lower in Beijing than those in the northeastern U.S. during the NEAQS study, whereas emission ratios of C8 aromatics are significantly higher in Beijing, possibly due to large emissions from industrial and/or solvent use emissions in Beijing and surrounding areas. Secondary formation from anthropogenic precursors was generally more important to reactive aldehydes than inert ketones and alcohols. Primary emissions accounted for the majority of the concentrations of ketones and alcohols. The differences found for allocation of OVOCs sources between Beijing and the NEAQS 2002 campaign are mainly attributable to the different atmospheric processing time in the two campaigns.

[49] PMF extracted four factors from the Beijing VOCs data set. The four factors were shown to be strongly influenced by photochemical processing as well as by the VOCs sources. They are identified representing fresh primary emissions, aged primary emissions, secondary formation and transport (secondary+transport) and biogenic emissions. The relative contributions of the three anthropogenic factors to NMHCs concentrations depended strongly on the k_{OH} values of NMHCs. The profiles of the three anthropogenic factors indicated that the fresh primary factor represented VOCs emissions without any photochemical degradation, while the other two anthropogenic factors were derived from the fresh primary factor by photochemical processing during a certain OH exposure. Though a biogenic factor was resolved from PMF, VOCs concentrations from anthropogenic and biogenic sources are not entirely separated. Although PMF explained more variability of VOCs concentrations than the parameterization method, the factors from PMF could not be attributed to specific sources classes.

[50] Our results show that photochemistry plays an important role in the results of PMF analyses. Variations in photochemical processing and varying of contributions from VOCs sources both lead to changes in concentrations and compositions of VOCs in the atmosphere. Photochemistry affects VOCs compositions through the large differences in OH reaction rates of various VOCs species. PMF algorithms are designed to find profiles and contributions for a certain number of factors that minimize the weighed residues in the data matrix. If the importance of photochemistry in the atmosphere exceeds differences of emission compositions from various sources, factors in PMF will also be extracted according to different degree of photochemical processing, not just based on the individual sources. The summer VOCs data set in Beijing clearly demonstrates the importance of photochemistry in PMF analysis. Even in the center of Beijing, a highly urbanized area surrounded by a very large and complex mix of VOC emission sources, the results of PMF analysis predominately separate degrees of photochemical processing rather than specific VOCs source categories. Since the photochemistry of VOCs is ubiquitous in the atmosphere, results of all PMF analyses, both future analyses and those already reported in the literature, must be carefully interpreted with full consideration of the influence of photochemistry. The exploration of factor characterization and factor independence presented in this paper can provide a guide for such interpretation. It will be quite interesting to investigate PMF results of VOCs measured in other environments or other seasons (e.g., winter) using the methods described in this study.

[51] **Acknowledgments.** This work is supported by China National Funds for Distinguished Young Scientists from NSFC (41125018). The authors would like to thank the valuable comments from the three anonymous reviewers.

References

Apel, E. C., et al. (2002), Measurement and interpretation of isoprene fluxes and isoprene, methacrolein, and methyl vinyl ketone mixing ratios at the PROPHET site during the 1998 Intensive, *J. Geophys. Res.*, *107*(D3), 4034, doi:10.1029/2000JD000225.

Atkinson, R., and J. Arey (2003a), Atmospheric degradation of volatile organic compounds, *Chem. Rev.*, *103*(12), 4605–4638, doi:10.1021/cr0206420.

Atkinson, R., and J. Arey (2003b), Gas-phase tropospheric chemistry of biogenic volatile organic compounds: A review, *Atmos. Environ.*, *37*, suppl. 2, 197–219, doi:10.1016/S1352-2310(03)00391-1.

Atkinson, R., D. L. Baulch, R. A. Cox, J. N. Crowley, R. F. Hampson, R. G. Hynes, M. E. Jenkin, M. J. Rossi, and J. Troe (2006), Evaluated kinetic and photochemical data for atmospheric chemistry: Volume II—Gas phase reactions of organic species, *Atmos. Chem. Phys.*, *6*, 3625–4055, doi:10.5194/acp-6-3625-2006.

Bon, D. M., et al. (2011), Measurements of volatile organic compounds at a suburban ground site (T1) in Mexico City during the MILAGRO 2006 campaign: Measurement comparison, emission ratios, and source attribution, *Atmos. Chem. Phys.*, *11*(6), 2399–2421, doi:10.5194/acp-11-2399-2011.

Buzcu, B., and M. P. Fraser (2006), Source identification and apportionment of volatile organic compounds in Houston, TX, *Atmos. Environ.*, *40*(13), 2385–2400, doi:10.1016/j.atmosenv.2005.12.020.

de Gouw, J., and C. Warneke (2007), Measurements of volatile organic compounds in the Earth's atmosphere using proton-transfer-reaction mass spectrometry, *Mass Spectrom. Rev.*, *26*(2), 223–257, doi:10.1002/mas.20119.

de Gouw, J. A., P. D. Goldan, C. Warneke, W. C. Kuster, J. M. Roberts, M. Marchewka, S. B. Bertman, A. A. P. Pszenny, and W. C. Keene (2003), Validation of proton transfer reaction-mass spectrometry (PTR-MS) measurements of gas-phase organic compounds in the atmosphere during the New England Air Quality Study (NEAQS) in 2002, *J. Geophys. Res.*, *108*(D21), 4682, doi:10.1029/2003JD003863.

de Gouw, J. A., et al. (2005), Budget of organic carbon in a polluted atmosphere: Results from the New England Air Quality Study in 2002, *J. Geophys. Res.*, *110*, D16305, doi:10.1029/2004JD005623.

de Gouw, J. A., et al. (2008), Sources of particulate matter in the northeastern United States in summer: 1. Direct emissions and secondary formation of organic matter in urban plumes, *J. Geophys. Res.*, *113*, D08301, doi:10.1029/2007JD009243.

Fujita, E. M. (2001), Hydrocarbon source apportionment for the 1996 Paso del Norte Ozone Study, *Sci. Total Environ.*, *276*(1–3), 171–184, doi:10.1016/S0048-9697(01)00778-1.

Gaimoz, C., et al. (2011), Volatile organic compounds sources in Paris in spring 2007. Part II: Source apportionment using positive matrix factorisation, *Environ. Chem.*, *8*(1), 91–103, doi:10.1071/EN10067.

Goldstein, A. H., S. M. Fan, M. L. Goulden, J. W. Munger, and S. C. Wofsy (1996), Emissions of ethene, propene, and *1*-butene by a midlatitude forest, *J. Geophys. Res.*, *101*(D4), 9149–9157, doi:10.1029/96JD00334.

Guenther, A. (2002), The contribution of reactive carbon emissions from vegetation to the carbon balance of terrestrial ecosystems, *Chemosphere*, *49*(8), 837–844, doi:10.1016/S0045-6535(02)00384-3.

Harley, R. A., S. C. Coulter-Burke, and T. S. Yeung (2000), Relating liquid fuel and headspace vapor composition for California reformulated gasoline samples containing ethanol, *Environ. Sci. Technol.*, *34*(19), 4088–4094, doi:10.1021/es0009875.

Hester, R. (1995), *Volatile Organic Compounds in the Atmosphere*, R. Soc. of Chem., London.

Hopke, P. (2000), A guide to positive matrix factorization, paper presented at Workshop on UNMIX and PMF as Applied to PM2.5, U.S. Environ. Prot. Agency, Research Triangle Park, N. C.

Jimenez, J. L., et al. (2009), Evolution of organic aerosols in the atmosphere, *Science*, *326*(5959), 1525–1529, doi:10.1126/science.1180353.

Kleinman, L. I., et al. (2003), Photochemical age determinations in the Phoenix metropolitan area, *J. Geophys. Res.*, *108*(D3), 4096, doi:10.1029/2002JD002621.

Koppmann, R. (Ed.) (2007), *Volatile Organic Compounds in the Atmosphere*, Blackwell, Oxford, U. K., doi:10.1002/9780470988657

Lanz, V. A., C. Hueglin, B. Buchmann, M. Hill, R. Locher, J. Staehelin, and S. Reimann (2008), Receptor modeling of C2–C7 hydrocarbon sources at an urban background site in Zurich, Switzerland: Changes between 1993–1994 and 2005–2006, *Atmos. Chem. Phys.*, *8*(9), 2313–2332, doi:10.5194/acp-8-2313-2008.

Latella, A., G. Stani, L. Cobelli, M. Duane, H. Junninen, C. Astorga, and B. R. Larsen (2005), Semicontinuous GC analysis and receptor modelling for source apportionment of ozone precursor hydrocarbons in Bresso, Milan, 2003, *J. Chromatogr. A*, *1071*(1–2), 29–39, doi:10.1016/j.chroma.2004.12.043.

Liu, X. L., L. M. Zeng, S. H. Lu, and X. N. Yu (2009), Online monitoring system for volatile organic compounds in the atmosphere, *Acta Sci. Circumstantiae*, *29*(12), 2471–2477.

Liu, Y., M. Shao, L. L. Fu, S. H. Lu, L. M. Zeng, and D. G. Tang (2008), Source profiles of volatile organic compounds (VOCs) measured in China: Part I, *Atmos. Environ.*, *42*(25), 6247–6260, doi:10.1016/j.atmosenv.2008.01.070.

Liu, Y., M. Shao, W. C. Kuster, P. D. Goldan, X. H. Li, S. H. Lu, and J. A. De Gouw (2009), Source identification of reactive hydrocarbons and oxygenated VOCs in the summertime in Beijing, *Environ. Sci. Technol.*, *43*(1), 75–81, doi:10.1021/es801716n.

Liu, Z., et al. (2012), Summertime photochemistry during CAREBeijing-2007: RO_x budgets and O_3 formation, *Atmos. Chem. Phys.*, *12*(16), 7737–7752, doi:10.5194/acp-12-7737-2012.

Lu, K., et al. (2010), Oxidant (O_3+NO_2) production processes and formation regimes in Beijing, *J. Geophys. Res.*, *115*, D07303, doi:10.1029/2009JD012714.

Lu, K. D., et al. (2012), Missing OH source in a suburban environment near Beijing: Observed and modelled OH and HO_2 concentrations in summer 2006, *Atmos. Chem. Phys. Discuss.*, *12*(4), 10,879–10,936, doi:10.5194/acpd-12-10879-2012.

McKeen, S. A., S. C. Liu, E. Y. Hsie, X. Lin, J. D. Bradshaw, S. Smyth, G. L. Gregory, and D. R. Blake (1996), Hydrocarbon ratios during PEM-WEST A: A model perspective, *J. Geophys. Res.*, *101*(D1), 2087–2109, doi:10.1029/95JD02733.

Morino, Y., T. Ohara, Y. Yokouchi, and A. Ooki (2011), Comprehensive source apportionment of volatile organic compounds using observational data, two receptor models, and an emission inventory in Tokyo metropolitan area, *J. Geophys. Res.*, *116*, D02311, doi:10.1029/2010JD014762.

Na, K. S., and Y. P. Kim (2007), Chemical mass balance receptor model applied to ambient C-2–C9 VOC concentration in Seoul, Korea: Effect of chemical reaction losses, *Atmos. Environ.*, *41*(32), 6715–6728, doi:10.1016/j.atmosenv.2007.04.054.

Norris, G., R. Vedantham, K. Wade, S. Brown, J. Prouty, and C. Foley (2008), EPA positive matrix factorization (PMF) 3.0 fundamentals and user guide, *Rep. EPA 600/R-08/108*, U.S. Environ. Prot. Agency, Washington, D. C.

Paatero, P. (1997), Least squares formulation of robust non-negative factor analysis, *Chemom. Intell. Lab. Syst.*, *37*(1), 23–35, doi:10.1016/S0169-7439(96)00044-5.

Pang, X. B., Y. J. Mu, Y. J. Zhang, X. Q. Lee, and J. Yuan (2009), Contribution of isoprene to formaldehyde and ozone formation based on its oxidation products measurement in Beijing, China, *Atmos. Environ.*, *43*(13), 2142–2147, doi:10.1016/j.atmosenv.2009.01.022.

Parrish, D. D., et al. (1998), Internal consistency tests for evaluation of measurements of anthropogenic hydrocarbons in the troposphere, *J. Geophys. Res.*, *103*(D17), 22,339–22,359, doi:10.1029/98JD01364.

Parrish, D. D., A. Stohl, C. Forster, E. L. Atlas, D. R. Blake, P. D. Goldan, W. C. Kuster, and J. A. de Gouw (2007), Effects of mixing on evolution of hydrocarbon ratios in the troposphere, *J. Geophys. Res.*, *112*, D10S34, doi:10.1029/2006JD007583.

Parrish, D. D., W. C. Kuster, M. Shao, Y. Yokouchi, Y. Kondo, P. D. Goldan, J. A. de Gouw, M. Koike, and T. Shirai (2009), Comparison of air pollutant emissions among mega-cities, *Atmos. Environ.*, *43*(40), 6435–6441, doi:10.1016/j.atmosenv.2009.06.024.

Roberts, J. M., F. C. Fehsenfeld, S. C. Liu, M. J. Bollinger, C. Hahn, D. L. Albritton, and R. E. Sievers (1984), Measurements of aromatic hydrocarbon ratios and NO_x concentrations in the rural troposphere: Observation of air mass photochemical aging and NO_x removal, *Atmos. Environ.*, *18*(11), 2421–2432.

Seinfeld, J. H., and S. N. Pandis (1998), *Atmospheric Chemistry and Physics: From Air Pollution to Climate Change*, John Wiley, Hoboken, N. J., doi:10.1063/1.882420.

Shao, M., S. H. Lu, Y. Liu, X. Xie, C. C. Chang, S. Huang, and Z. M. Chen (2009), Volatile organic compounds measured in summer in Beijing and their role in ground-level ozone formation, *J. Geophys. Res.*, *114*, D00G06, doi:10.1029/2008JD010863.

Shao, M., B. Wang, S. Lu, B. Yuan, and M. Wang (2011), Effects of Beijing Olympics control measures on reducing reactive hydrocarbon species, *Environ. Sci. Technol.*, *45*(2), 514–519, doi:10.1021/es102357t.

Shim, C. S., Y. H. Wang, H. B. Singh, D. R. Blake, and A. B. Guenther (2007), Source characteristics of oxygenated volatile organic compounds and hydrogen cyanide, *J. Geophys. Res.*, *112*, D10305, doi:10.1029/2006JD007543.

Slowik, J. G., A. Vlasenko, M. McGuire, G. J. Evans, and J. P. D. Abbatt (2010), Simultaneous factor analysis of organic particle and gas mass spectra: AMS and PTR-MS measurements at an urban site, *Atmos. Chem. Phys.*, *10*(4), 1969–1988, doi:10.5194/acp-10-1969-2010.

Song, Y., M. Shao, Y. Liu, S. H. Lu, W. Kuster, P. Goldan, and S. D. Xie (2007), Source apportionment of ambient volatile organic compounds in Beijing, *Environ. Sci. Technol.*, *41*(12), 4348–4353, doi:10.1021/es0625982.

Song, Y., W. Dai, M. Shao, Y. Liu, S. H. Lu, W. Kuster, and P. Goldan (2008), Comparison of receptor models for source apportionment of volatile organic compounds in Beijing, China, *Environ. Pollut.*, *156*(1), 174–183, doi:10.1016/j.envpol.2007.12.014.

Streets, D. G., et al. (2007), Air quality during the 2008 Beijing Olympic Games, *Atmos. Environ.*, *41*(3), 480–492, doi:10.1016/j.atmosenv.2006.08.046.

Stroud, C. A., et al. (2001), Isoprene and its oxidation products, methacrolein and methylvinyl ketone, at an urban forested site during the 1999 Southern Oxidants Study, *J. Geophys. Res.*, *106*(D8), 8035–8046, doi:10.1029/2000JD900628.

Ulbrich, I. M., M. R. Canagaratna, Q. Zhang, D. R. Worsnop, and J. L. Jimenez (2009), Interpretation of organic components from Positive Matrix Factorization of aerosol mass spectrometric data, *Atmos. Chem. Phys.*, *9*, 2891–2918, doi:10.5194/acp-9-2891-2009.

Vlasenko, A., et al. (2009), Measurements of VOCs by proton transfer reaction mass spectrometry at a rural Ontario site: Sources and correlation to aerosol composition, *J. Geophys. Res.*, *114*, D21305, doi:10.1029/2009JD012025.

Vlasenko, A., A. M. Macdonald, S. J. Sjostedt, and J. P. D. Abbatt (2010), Formaldehyde measurements by proton transfer reaction–mass spectrometry (PTR-MS): Correction for humidity effects, *Atmos. Meas. Tech.*, *3* (4), 1055–1062, doi:10.5194/amt-3-1055-2010.

von Schneidemesser, E., P. S. Monks, and C. Plass-Duelmer (2010), Global comparison of VOC and CO observations in urban areas, *Atmos. Environ.*, *44*(39), 5053–5064, doi:10.1016/j.atmosenv.2010.09.010.

Wang, B., M. Shao, S. H. Lu, B. Yuan, Y. Zhao, M. Wang, S. Q. Zhang, and D. Wu (2010a), Variation of ambient non-methane hydrocarbons in Beijing city in summer 2008, *Atmos. Chem. Phys.*, *10*(13), 5911–5923, doi:10.5194/acp-10-5911-2010.

Wang, B., M. Shao, J. M. Roberts, G. Yang, F. Yang, M. Hu, L. Zeng, Y. Zhang, and J. Zhang (2010b), Ground-based on-line measurements of peroxyacetyl nitrate (PAN) and peroxypropionyl nitrate (PPN) in the Pearl River Delta, China, *Int. J. Environ. Anal. Chem.*, *90*(7), 548–559, doi:10.1080/03067310903194972.

Wang, T., A. J. Ding, J. Gao, and W. S. Wu (2006), Strong ozone production in urban plumes from Beijing, China, *Geophys. Res. Lett.*, *33*, L21806, doi:10.1029/2006GL027689.

Warneke, C., et al. (2007), Determination of urban volatile organic compound emission ratios and comparison with an emissions database, *J. Geophys. Res.*, *112*, D10S47, doi:10.1029/2006JD007930.

Warneke, C., et al. (2011), Airborne formaldehyde measurements using PTR-MS: Calibration, humidity dependence, inter-comparison and initial results, *Atmos. Meas. Tech.*, *4*(10), 2345–2358, doi:10.5194/amt-4-2345-2011.

Watson, J. G., J. C. Chow, and E. M. Fujita (2001), Review of volatile organic compound source apportionment by chemical mass balance, *Atmos. Environ.*, *35*(9), 1567–1584, doi:10.1016/S1352-2310(00)00461-1.

Xiao, Y. P., J. A. Logan, D. J. Jacob, R. C. Hudman, R. Yantosca, and D. R. Blake (2008), Global budget of ethane and regional constraints on U.S. sources, *J. Geophys. Res.*, *113*, D21306, doi:10.1029/2007JD009415.

Xie, X., M. Shao, Y. Liu, S. Lu, C.-C. Chang, and Z.-M. Chen (2008), Estimate of initial isoprene contribution to ozone formation potential in Beijing, China, *Atmos. Environ.*, *42*(24), 6000–6010, doi:10.1016/j.atmosenv.2008.03.035.

Yuan, B., M. Shao, S. Lu, and B. Wang (2010), Source profiles of volatile organic compounds associated with solvent use in Beijing, China, *Atmos. Environ.*, *44*(15), 1919–1926, doi:10.1016/j.atmosenv.2010.02.014.

Zhang, Q., et al. (2009), Asian emissions in 2006 for the NASA INTEX-B mission, *Atmos. Chem. Phys.*, *9*(14), 5131–5153, doi:10.5194/acp-9-5131-2009.